Lithological Control on Scour Hole Formation in the Rhine-Meuse Estuary

Ymkje Huismans[1], Hilde Koopmans[1,2], Ane Wiersma[1], Tjalling de Haas[3], Koen Berends[1],

Kees Sloff[1,2] and Esther Stouthamer[3]

[1]Deltares, P.O. Box 177, 2600 MH Delft, the Netherlands.

[2]Faculty of Civil Engineering and Geosciences, Delft University of Technology, P.O. Box 5048, 2600 GA Delft, the Netherlands.

[3]Faculty of Geosciences, Utrecht University, P.O. Box 80115, 3508 TC Utrecht, the Netherlands.

Corresponding author: Ymkje Huismans (Ymkje.Huismans@deltares.nl)

Abstract

River deltas commonly have a heterogeneous substratum of alternating peat, clay and sand deposits. This has important consequences for the river bed development and in particular for scour hole formation. When the substratum consists of an erosion resistant top layer, erosion is retarded. Upon breaking through a resistant top layer and reaching an underlying layer with higher erodibilty, deep scour holes may form within a short amount of time. The unpredictability and fast development of these scour holes makes them difficult to manage, particularly where the stability of dikes and infrastructure is at stake.

In this paper we determine how subsurface lithology controls the bed elevation in net incising river branches, particularly focusing on scour hole initiation, growth rate, and direction. For this, the

Rhine-Meuse Estuary forms an ideal study site, as over 100 scour holes have been identified in this area, and over 40 years of bed level data and thousands of core descriptions are available. It is shown that the subsurface lithology plays a crucial role in the emergence, shape, and evolution of scour holes. Although most scour holes follow the characteristic exponential development of fast initial growth and slower final growth, strong temporal variations are observed, with sudden growth rates of several meters per year in depth and tens of meters in extent. In addition, we relate the characteristic build-up of the subsurface lithology to specific geometric characteristics of scour holes, like large elongated expanding scour holes or confined scour holes with steep slopes. As river deltas commonly have a heterogeneous substratum and often face channel bed erosion, the observations likely apply to many delta rivers. These findings call for thorough knowledge of the subsurface lithology, as without it, scour hole development is hard to predict and can lead to sudden failures of nearby infrastructure and flood defence works.

Keywords: Scour holes, morphology, geology, delta rivers

1 Introduction

Scour holes are common features in rivers and estuaries. With their steep slopes and large depths, these scour holes can threaten the stability of nearby infrastructure like embankments, bridge piers, tunnels and pipelines (e.g. Gharabaghi et al., 2007; Beltaos et al., 2011; Wang et al., 2017; Pandey et al., 2018; Liang et al., 2020). The formation and development of local scour, bend scour, and confluence scour are widely studied (e.g., Engelund, 1974; Mosley, 1976; Zimmermann & Kennedy, 1978; Kjerfve et al., 1979; Odgaard, 1981; Best, 1986; Andrle, 1994; Ginsberg & Perillo, 1999; Pierini et al., 2005; Gharabaghi et al., 2007; Best & Rhoads, 2008; Blanckaert, 2010;

43 Beltaos et al., 2011; Ottevanger et al., 2012; Vermeulen et al., 2015; Wang et al., 2017; Ferrarin

44 et al., 2018; Pandey et al., 2018; Liang et al., 2020). These studies however generally focus on

45 scour hole development in a homogeneous sandy subsurface. The influence of heterogeneities in

46 the subsurface lithology on scour hole formation is hardly studied, although this may greatly

47 impact the scour hole evolution or even induce scour hole formation (Fig. 1), provided there is

48 enough hydraulic forcing. In case of large-scale bed degradation in channel beds composed of

49 fluvial sand and with no constructions or local river narrowing, erosion is evenly distributed.

50 However, when the substratum is composed of layers with strongly varying erodibility, local

51 depressions form at locations with higher erodibility (Cserkész-Nagy et al. 2010; Sloff et al. 2013;

52 Huismans et al. 2016).

53   Many of world's large rivers in deltas face channel bed degradation, such as the Yangtze,

54 the Rhine-Meuse Estuary, the Mississippi and the Mekong rivers (Galler et al. 2003; Sloff et al.

55 2013; Brunier et al. 2014; Luan et al. 2016; Hoitink et al. 2017; Wang and Xu 2018). The causes

56 of this degradation are mainly anthropogenic and range from extracting sediment by dredging and

57 sand mining, to a reduction in sediment supply due to the presence of upstream dams, or to levees

58 and interventions that enhance flow velocities. As river deltas commonly have a heterogeneous

59 substratum of alternating peat, clay, and sand deposits (e.g. Aslan & Autin, 1999; Berendsen &

60 Stouthamer, 2001, 2002; Aslan et al., 2005; Kuehl et al., 2005.; Stefani & Vincenzi, 2005; Gouw

61 & Autin, 2008; Cohen et al., 2012; Hanebuth et al., 2012), and are among the regions with the

62 highest population density (Syvitski et al. 2009; Best 2019), understanding how lithology controls

63 the scour hole development is highly relevant to sustainable river management.

64   A detailed analysis of the influence of a heterogenous subsurface lithology on the

65 general channel bed morphology is carried out by Nittrouer et al. (2011). Based on multibeam

surveys, high intensity radar pulse seismic data, and grab samples, they map five sediment facies for the lowermost Mississippi river, three of which consist of modern alluvial deposits, and two of relict substratum. They show that the sediment facies associated with relict substratum are mainly exposed in the regions with the most erosion, namely the deeper parts of the channel bed and at the sidewalls of the outer bends. Erosion of the sidewall substratum is furthermore inhomogeneous, due to the spatially heterogeneous fluvio-deltaic sedimentary deposits that have variable resistance to erosion. The heterogeneous

channel deposits are furthermore found to influence the depth of meander pools in the Lower Mississippi river (Hudson, 2002; Gibson et al., 2019). Cserkész-Nagy et al. (2010) show a strong lithological control on the erosion and lateral migration of the Tisza river (Hungary) in response to engineering measures. Erosion is either found to be promoted, in case sandy deposits are incised, or suppressed when resistant silty-clayey substratum prohibits further erosion. For the Ems estuary, Pierik et al. (2019) demonstrate how the composition of the subsurface lithology controlled the evolution of ebb-tidal channels over a 200 years timespan. The clear link to the emergence of scour holes is made by Sloff et al. (2013), who observed deep scour holes in the Rhine-Meuse estuary and demonstrated the principle of scour hole formation in heterogeneous subsurfaces both conceptually and with a numerical model. In an exploratory study by Huismans et al. (2016), the link between scour hole occurrence and the composition of the subsurface lithology was made directly by combining multibeam surveys with detailed geological maps constructed based on lithological data from corings.
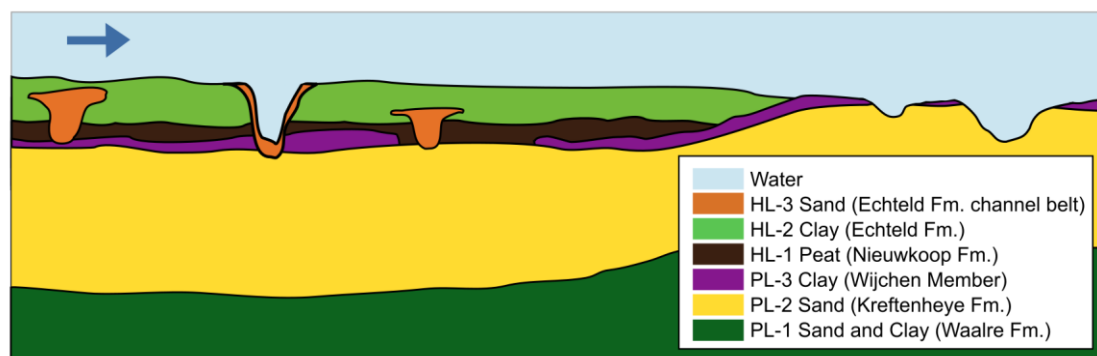
86

Figure 1. Conceptual longitudinal subsurface lithological longitudinal section of a river bed, with typical distances of 10 to 20 meters in depth and 10 to 20 km in length. Arrow indicates flow direction. In colour the lithological formations (Fm.) and members are indicated. Scour holes form in layers or patches composed of sandy material with lower erodibility compared to the surrounding resistant clay or peat layers.

The influence of lithology on the time- and spatial evolution of scour holes has never been studied. In this paper we analyse in detail how the subsurface lithology influences the bed elevation in net incising river branches. We focus on scour hole initiation, growth rate, direction and shape, as this is essential information in judging whether scour holes form a risk for the stability of river banks, dikes or other nearby infrastructure. We hypothesise that the lithology can trigger scour hole formation and that it can be a dominant factor in controlling the growth rates and shape.

The Rhine-Meuse Estuary in the Netherlands forms an ideal study area, as more than a hundred scour holes are identified in this area, of which many are expected to be influenced or triggered by heterogeneities in the subsurface lithology (Huismans et al., 2016). In addition, over 40 years of yearly single- and multibeam surveys and lithological data from many corings are available. This allows the analysis of decades of bed level evolution and linking it to the subsurface composition. Because much fewer scour holes are found upstream from the tidally- influenced Rhine Meuse Estuary and the subsurface lithology is less heterogeneous, this study focusses on

105 the Rhine Meuse Estuary and is not extended further upstream. Upon identifying how the location,

106 growth direction and rates are influenced by the heterogeneity of the subsurface lithology, first a

107 reconstruction of the subsurface lithology is made based on thousands of core descriptions along

108 the main river branches of the Rhine-Meuse Estuary. Subsequently, the recent five-year scour hole

109 growth is mapped for the set of over 100 scour holes. For a subset of 18 scour holes, the evolution

110 since 1976 is analysed and linked to the subsurface lithology. In a final step, scour hole

111 characteristics in two sub-reaches with distinct lithological composition are analysed, highlighting

112 the differences in lithological control on the size, growth rate and direction of scour holes.

113 **2 Study Area**

114   The Rhine-Meuse Estuary is located in the western part of the Netherlands, where the rivers

115 Rhine and Meuse debouch into the North Sea (Fig. 2). During the Late Pleistocene Younger Dryas

116 stadial (12.900-11.700 cal yr. BP), the area consisted of a braided river valley. During the early

117 Holocene (11.700 - 8.200 cal yr. BP), the braided river system gradually transformed into a

118 meandering system, due to climatic warming and restoration of vegetation (Pons, 1957; Berendsen

119 et al., 1995; Berendsen & Stouthamer, 2000; Cohen, 2003; Gouw & Erkens, 2007; Hijma, 2009;

120 Janssens et al., 2012). The sandy sediments deposited by the braided rivers predominantly consist

121 of gravel and coarse sand (Kreftenheye Fm., PL-2, Fig. 1). At the top of these deposits finer grained

122 sand is found, with grain sizes varying from 150 µm to 300 µm (Vos & Cohen, 2014). During

123 flood events, fine-grained sediments were deposited on the floodplains, forming a resistant silty

124 clay layer (Wijchen Member, PL-3) (Törnqvist et al. 1994; Busschers et al. 2007; Hijma et al.

125 2009). In most of the study area, this silty clay layer (Wijchen Mb.) covers the Pleistocene sandy

126 deposits (PL-2). Due to rapid early Holocene sea level rise, the area changed from a wide river

127 valley into an estuary (De Haas et al., 2018; Hijma, 2009). During this stage peat lands formed in

128   response to the higher ground water tables (Nieuwkoop Fm., HL-1), which became regionally

129   covered by clay from tidal deposits in the west (Naaldwijk Fm.) and floodplain deposits in the east

130   (Echteld Fm., HL-2) (Hijma et al., 2009). The rapid growth in accommodation space triggered a

131   peak in avulsion frequency around 8000 – 7200 cal yr. BP (Stouthamer & Berendsen, 2000;

132   Stouthamer et al., 2011a). A second peak in avulsion frequency occurred around

133   3300-1800 cal yr. BP and was triggered from upstream, where due to deforestation sediment

134   supply to the river increased (Stouthamer & Berendsen, 2000; Erkens, 2009). During this time, a

135   major avulsion caused the Rhine to shift its mouth from the area near Leiden to the south near

136   Rotterdam, close to its current outlet position (Fig. 3a) (Berendsen & Stouthamer, 2000; Pierik et

137   al., 2018; De Haas et al., 2019). A detailed geological mapping of the past river course

138   development is available for the entire Rhine-Meuse Delta (Cohen et al., 2012), showing where

139   the river and tidal channel deposits are preserved in the subsurface lithology (HL-3).
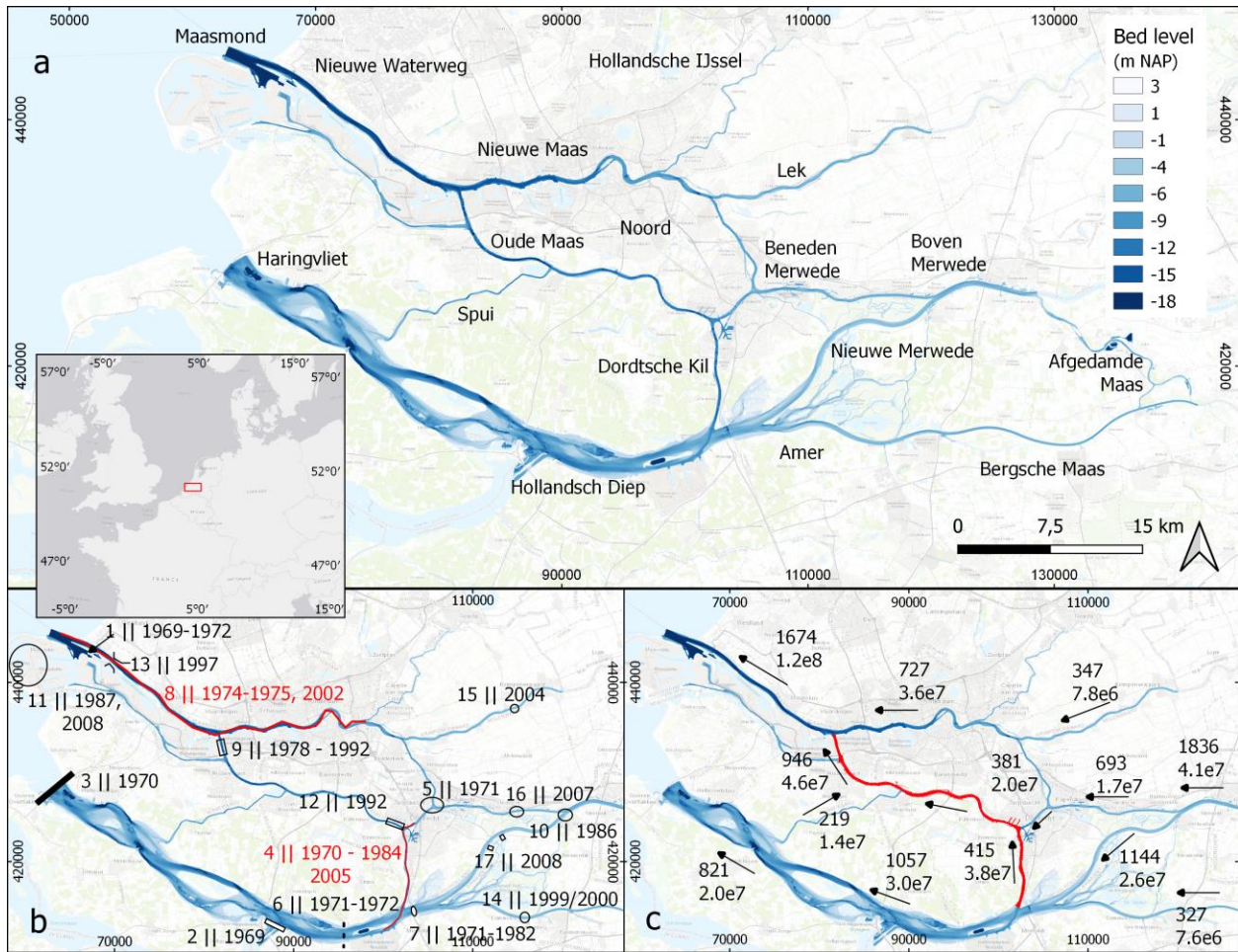
Figure 2 a) Overview of the river channels forming the Rhine-Meuse Estuary (the Netherlands). In colour the bed level is represented (year 2013, 2014). Coordinates in Amersfoort/ RD-new. The inset shows the location of the study area in NW-Europe. b) Overview of the most relevant engineering modifications since 1970, with details in table 1. c) Overview of averaged values of net river discharges (top numbers, in m^3/s) and tidal volumes (lower numbers, in m^3), from a one-dimensional numerical-model simulation for the year 2013 (Cox et al., submitted). The branches that are studied in more detail in this paper are indicated in red. Maps are created in QGIS with the Esri-TOPO base map and Esri-Grey (light) base map (inset).

149   *Table 1. Overview of the most relevant engineering measures since 1969* (Rijkswaterstaat, 2005; Sloff et al., 2011).

Year	no	branch	Measure
1969-1972	1	Nieuwe Waterweg	Construction of a dam between Nieuwe Waterweg and the access channel to Europoort.
1969	2	Hollandsche Diep	Closure Volkerak from Hollandsch Diep with a dam and ship locks.
1970	3	Haringvliet	Closure Haringvliet with sluices.
1970-1984	4	Dordtsche Kil/ Hollandsch Diep/ Oude Maas	Reconstruction Dordtsche Kil and deepening navigation channel (-8 m NAP).
1971	5	Beneden Merwede	Adjustment bifurcation with Noord and Oude Maas.
1971-1972	6	Hollandsche Diep	Construction of pipelines.
1971-1982	7	Hollandsche Diep	Dumping of sediment in deeper parts between Moerdijkbridges.
1974-1975	8	Nieuwe Waterweg, Nieuwe Maas	Construction "Trapjeslijn" a staircased bed with a stepwise increasing bed level.
1978 - 1993	9	Oude Maas	Construction of dams in the river bed (1978), filling up of deeper parts (1985-1986) and removal of two of the dams (1993).
1986	10	Nieuwe Merwede	Construction Beatrixhaven (Werkendam)
1987	11	Maasmond/ offshore	Construction of sludge depot Slufter
1992	12	Oude Maas	Shortening of groynes
1997	13	Nieuwe Waterweg	Construction storm surge barrier "Maeslantkering" finalised
1999-2000	14	Amer	Adjustment connection Wilhelminakanaal and Amer
2000, 2002	7	Nieuwe Waterweg, Nieuwe Maas	Deepening Trapjeslijn between km 1005 and 1013
2004	15	Lek	Bed cut-off, right bank near Bergambacht
2005	3	Dordtsche Kil/ Hollandsch Diep	Deepening navigation channel (-9.4 m NAP)
2007	16	Beneden Merwede	Construction open connection with polders
2008	11	Maasmond/ offshore	Start of construction "Tweede Maasvlakte".
2008	17	Nieuwe Merwede	Open connection Spieringpolders and polder Hardenhoek

150

151   Since the onset of the High Middle Ages (~1000 AD), human impacts on the delta

152 increased. Floodplains were cultivated, parts of the peat land excavated, and rivers were constraint

153 by dikes. This was followed by major changes to the river planform, when in the second half of

154 the 19th century, two new channels were constructed, the Nieuwe Merwede and Nieuwe Waterweg

155 (Fig. 2). Since that time, continuous deepening of channels, construction of groynes and

156 longitudinal dams (~1850-1920), and closure or reconstruction of river branches impacted the

157 Rhine-Meuse Estuary. An overview of the most relevant interventions since 1969 is given in

158   Figure 2b and Table 1. The measure which had the largest impact on the system as a whole is the

159   closure of one of its tidal outlets in 1970, the Haringvliet (no. 3, Table 1). The closure caused a

160   major change in the hydrodynamics (Vellinga et al., 2014), leading to enhanced flow velocities in

161   the connecting channels which triggered erosion of the river bed (Hoitink et al. 2017; Sloff et al.,

162   2013) of up to several meters in about 40 years' time (this paper). In the southern part of the

163   estuary, flow velocities strongly decreased, which resulted in sedimentation of mostly fine silt. To

164   keep the navigation channels open, an average of about 1.7 Mm^3 of sediment per year was dredged

165   between 2000-2018 (Cox et al., submitted). At present, most dredging occurs in the northern

166   channels (1.09 Mm^3/year), the Merwedes (0.37 Mm^3/year) and the Hollandsche Diep (0.20

167   Mm^3/year). In the connecting channels, only limited amount of dredging is carried out

168   (0.04 Mm^3/year).

169   The hydrodynamics in the Rhine Meuse Estuary are driven by a combination of river

170   discharge and tide (Fig. 2c). From upstream the system is fed by three rivers, the Lek, Waal, and

171   Meuse. During normal conditions, the dominant discharge route is through the Nieuwe Merwede,

172   Dordtsche Kil and Oude Maas to the Nieuwe Waterweg and Maasmond, which forms the main

173   outlet. During high river discharges, the net river discharge entering the system can reach up to

174   about 10,000 m^3/s, while during dry periods it may drop below 600 m^3/s. During low discharge

175   events, the Haringvliet sluices completely close, and all water leaves the system via the Maasmond

176   to limit salt intrusion in the Maasmond and ensure the fresh water supply in the estuary. The tidal

177   influence decreases landwards. Due to closure, the tidal volumes in Hollandsche Diep and

178   Haringvliet have dimished, and are small compared to their dimensions. In Table 2, details on the

179   net discharges and ebb- and flood velocities are given for the Dordtsche Kil and Oude Maas, the

180   two branches for which we analyse historic scour hole growth in relation to their geology.

181 *Table 2. Overview of the velocity (v) and discharge (Q) conditions for the Oude Maas and Dordtsche Kil river. As no*

182 *continuous measurements are available, values are extracted from a one dimensional numerical-model simulation for*

183 *the year 2013.*

Branch	v average (m/s)		v 90 percentile (m/s)		v max (m/s)		Q (m³/s)
	ebb	flood	ebb	flood	ebb	flood	
Dordtsche Kil	0.65-0.72	0.63-0.73	0.98-1.09	0.87-1.02	1.24-1.36	1.15-1.39	415
Oude Maas (between Dordtsche Kil and Spui)	0.49-0.80	0.30-0.53	0.69-1.09	0.50-0.85	0.96-1.45	0.78-1.25	727
Oude Maas (between Spui and Nieuwe Waterweg)	0.62-0.83	0.39-0.55	0.88-1.18	0.63-0.88	1.33-1.72	1.06-1.43	946

184

185   The Rhine-Meuse Estuary receives sediment from both the North Sea and its upstream

186 river branches Waal, Lek and Maas. The marine input of sand, silt and clay is estimated at

187 5.8 Mt/year, while only 1.3 Mt/year of sediment is exported to sea (Frings et al., 2019). Though

188 these numbers have a large uncertainty, the marine input is certainly large compared to the

189 combined input of all upstream river branches, which is 2.6 Mt/year (Frings et al., 2019). These

190 numbers show the system has a natural trend to import sediment. However, as dredging exceeds

191 the sediment import, the Rhine-Meuse Estuary has a net loss of sediment (Cox et al., submitted).

192   The genesis of the delta area with avulsions, infilling and abandoning channels and

193 development of marshes, has resulted in a heterogeneous substratum composed of clay and peat

194 layers and encased channel belts of sand. The grain size distribution and other sediment

195 characteristics of the top layer of the channel bed, vary strongly within the system. In the easterly

196 branches (Beneden Merwede, Nieuwe Merwede, Lek, Bergsche Maas), the channel bed is mostly

197 sandy, with median grain sizes ranging from 0.25 to 4 mm (Fugro, 2002; Frings et al., 2019).

198 Locally, the channel bed consists of erosion-resistant peat or clay. In the southern part (Haringvliet,

199 Hollandsch Diep, Amer), silt and clay fractions dominate the bed, of which most has settled since

200 the closure of the Haringvliet by a gated barrier in 1970. In the connecting branches (Oude Maas,

201 Noord, Dordtsche Kil, Spui), large areas of erosion resistant clay and peat form the channel bed,

202 but also areas with sand or silt are found (Fugro, 2002; Frings et al., 2019). In the Oude Maas, the

203 channel bed is mostly composed of clay from the Naaldwijk Fm. and Wijchen Mb., and sand from

204 the Kreftenheye Fm. In the Oude Maas reach between the confluences with the Dordtsche Kil and

205 Spui, Basal peat is occasionally found at the channel bed. In the Dordtsche Kil, the channel bed is

206 mostly composed of clay from the Echteld Fm. and sand from the Kreftenheye Fm.

207 **3 Data and methods**

208 To investigate the influence of the subsurface lithology on scour hole initiation, growth

209 rate and direction, an extensive set of geological data and bed level data is analysed. The method

210 consists of analysing and interpreting the geological records to reconstruct the subsurface lithology

211 and analysing single and multi-beam surveys to evaluate the bed level evolution and scour hole

212 growth in relation to the lithology. The subsurface lithology reconstruction resulted in lithological

213 longitudinal sections along the centrelines of most of the river branches. The data-analysis of the

214 bed level surveys is carried out in three phases. First, we created a general overview by mapping

215 the recent five-year growth characteristics for all scour holes in the estuary. Secondly, we analysed

216 the evolution of the overall bed level since 1976 for two branches, as well as the growth rates of

217 their scour holes. The observed trends are linked to the subsurface lithology. In the last step, we

218 analysed two sets of distinct scour holes in full detail. These two sets of scour holes differ in

219 growth rate, growth direction, and size, which can be related to differences in surrounding

220 geological layers.

221

222 3.1 Subsurface lithology

223   The main source of geological data is a digital database with lithological core descriptions

224   (Dino-database: TNO-Geological Survey of the Netherlands, 2010, 2014). For the area of interest,

225   core descriptions from within a range of 2 km of the river channel were selected (Fig. 3). Most

226   descriptions are from cores adjacent to the river channel. For the river branches Dordtsche Kil,

227   Nieuwe Maas, Boven Merwede and the Nieuwe Waterweg about 684 lithological core descriptions

228   and grab samples taken within the river are available. In addition to the core descriptions, the

229   Digital Basemap for Delta evolution and Paleogeography of the Rhine-Meuse Delta (Cohen et al.,

230   2012) is used for the location and age of the channel belts. The mapping of the channel belts is

231   based on cores from Utrecht University and the DINO-database, lidar imagery (www.ahn.nl), and

232   sedimentological and geomorphological principles. The dating is based on a combination of

233   archaeological findings, C14-dating, historical sources and maps, and geological cross-cutting

234   principles.

235   Based on the core descriptions, cone penetration tests, channel belt mapping and previous

236   paleogeographic reconstruction of the delta (Hijma & Cohen, 2011; Hijma et al., 2009), we

237   constructed lithological cross-sections and longitudinal sections for the Nieuwe Waterweg,

238   Nieuwe Maas, Oude Maas, Noord, Dordtsche Kil, Spui, Merwedes, and Lek (more details in the

239   reports by Stouthamer & De Haas, 2011; Stouthamer et al., 2011b-d; Huismans et al., 2013;
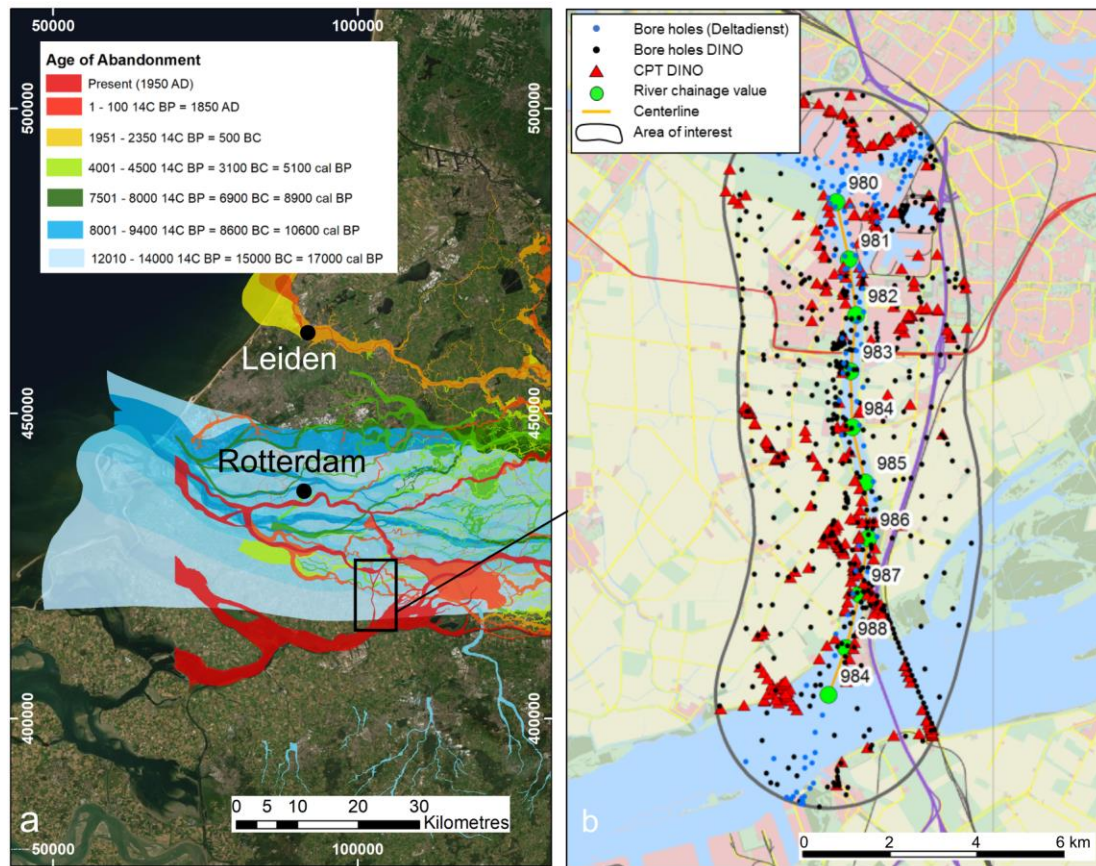
240   Wiersma, 2015).

Figure 3 Overview of the main data sources used for the reconstruction of the subsurface lithology, a) overview of the age of abandonment of Holocene channel belts (Cohen et al., 2012), map created with ArcGIS and with World Imagery used as background (Esri, Maxar, Earthstar Geographics, CNES/Airbus DS, USDA FSA, USGS, Aerogrid, IGN, IGP, and the GIS User Community), b) overview of the available core descriptions and cone penetration tests for the Dordtsche Kil river (Wiersma, 2015).

3.2 Bed level

For the analysis of the bed level evolution, single beam data is available for the period 1976 – 2005, and multibeam surveys are available from 2006 onwards, all provided by the Dutch Directorate-General for Public Works and Water Management. For the period 1976 – 1993, the single-beam data consists of yearly cross-sections at every 100 m to 125 m, with 10 m spacing between each measurement point within each cross-section. For the period 1994 – 1999, cross

253   sections are measured at every 25 m to 100 m with generally 1 m spacing between each

254   measurement point within the cross section. During this period, some areas were surveyed more

255   intensively with both cross and longitudinal sections. From the year 2000 the resolution increases

256   and the provided single beam measurements are interpolated onto a 5 x 5 m grid. The multi-beam

257   data from 2006 onwards consist of yearly surveys and are available on a 1 x 1 m resolution grid.

258   For areas that are surveyed more frequently, the last measured value is taken.

259   In the first step of the analysis, the growth characteristics over the period 2009 - 2014 are

260   determined for all scour holes identified in the study of Huismans et al. (2016). The scour holes

261   are detected by visual inspection of the bed topography of 2012. The database is available at

262   Mendeley Data and excludes groyne scour holes, as these develop by local turbulence from the

263   groynes. The groyne scour holes are therefore not typical for the Rhine-Meuse estuary. The

264   database consists of 81 scour holes, or groups of scour holes if they are located close to each other.

265   In the analysis all individual scour holes are regarded, such that in total 107 scour holes are

266   analysed. Due to insufficient bed topography data for the river branches Haringvliet and

267   Brabantsche Biesbosch, the scour holes in those branches were left out from the growth analysis.

268   Based on the multi-beam measurements from 2009 and 2014 the change in extent and depth over

269   five years' time is determined. The change in depth is defined as the difference between the level

270   of the deepest point in 2009 and 2014. Note that the location of the deepest point may change over

271   time. The change in extent is based on the evolution of the depth contour that marks the area of

272   the scour hole.

273   To analyse the decadal evolution of the scour hole growth in relation to the geology, we

274   focus on two branches, the Dordtsche Kil and Oude Maas. These branches were selected as they

275   face a strong overall bed degradation and have the most comprehensive datasets regarding geology

276   and bed level surveys. For these branches the bed level evolution from 1976 to present is analysed,

277   by plotting the maximum depth along the river. For each river km interval, the deepest point over

278   the width of the river is determined (thalweg). For the single beam measurements, the maximum

279   depth per measured cross-section is taken, which results in resolutions ranging between 25 m to

280   125 m, depending on the spacing of the original single beam tracks. For the interpolated single

281   beam and multibeam data, the thalweg has a resolution of 100 m for 2000 and 2004 and 10 m for

282   all other years.

283   To evaluate the depth development of the scour holes of the Dordtsche Kil and Oude Maas

284   between 1976 and 2015, the deepest point within the scour hole is plotted against time. This

285   enables to determine whether a scour hole grows steadily in depth or whether it faces a sudden

286   acceleration or deceleration in growth, and whether the depth is stabilising. Because the size of the

287   scour holes may be comparable to the distance between the various single beam cross-sections,

288   only points within a range of 50 m from the current deepest point of the scour hole are considered.

289   In the last step of the analysis, we analyse two reaches in full detail. To determine the length-width

290   ratio of the scour holes, the smallest possible rectangle is fitted around each scour hole. The

291   elevation of the scour hole edge is inferred from the elevation profile. The elevation at which the

292   inflection point is located is regarded as the scour hole edge. In some cases the slope changes

293   gradually and no clear inflection point is present. For these cases the elevation at which the bed

294   becomes horizontal is taken as the scour hole edge.

295   **4 Results**

296   4.1 Recent growth characteristics of all scour holes

297   An overview of the scour holes in the Rhine-Meuse Estuary is given in Figure 4, together

298   with the bed level trends, as taken from the most recent sediment budget of the Rhine-Meuse

299   Estuary (Becker, 2015) for the period 2002-2012. Scour holes are found in all river channels

300   throughout the entire delta, even in branches that are aggrading. Scour holes in these branches are

301   presumably related to either the presence of structures like bridge piers, which cause local scour,

302   or are relics of old tidal channels that have not been infilled yet.

303   The overview of the scour hole development between 2009-2014 (Fig. 4), shows that most

304   of the scour holes still grow in depth or extent. Only about 10% of the scour holes shows a depth

305   increase of more than 50 cm or an increase in extent of more than 50% over five years' time.
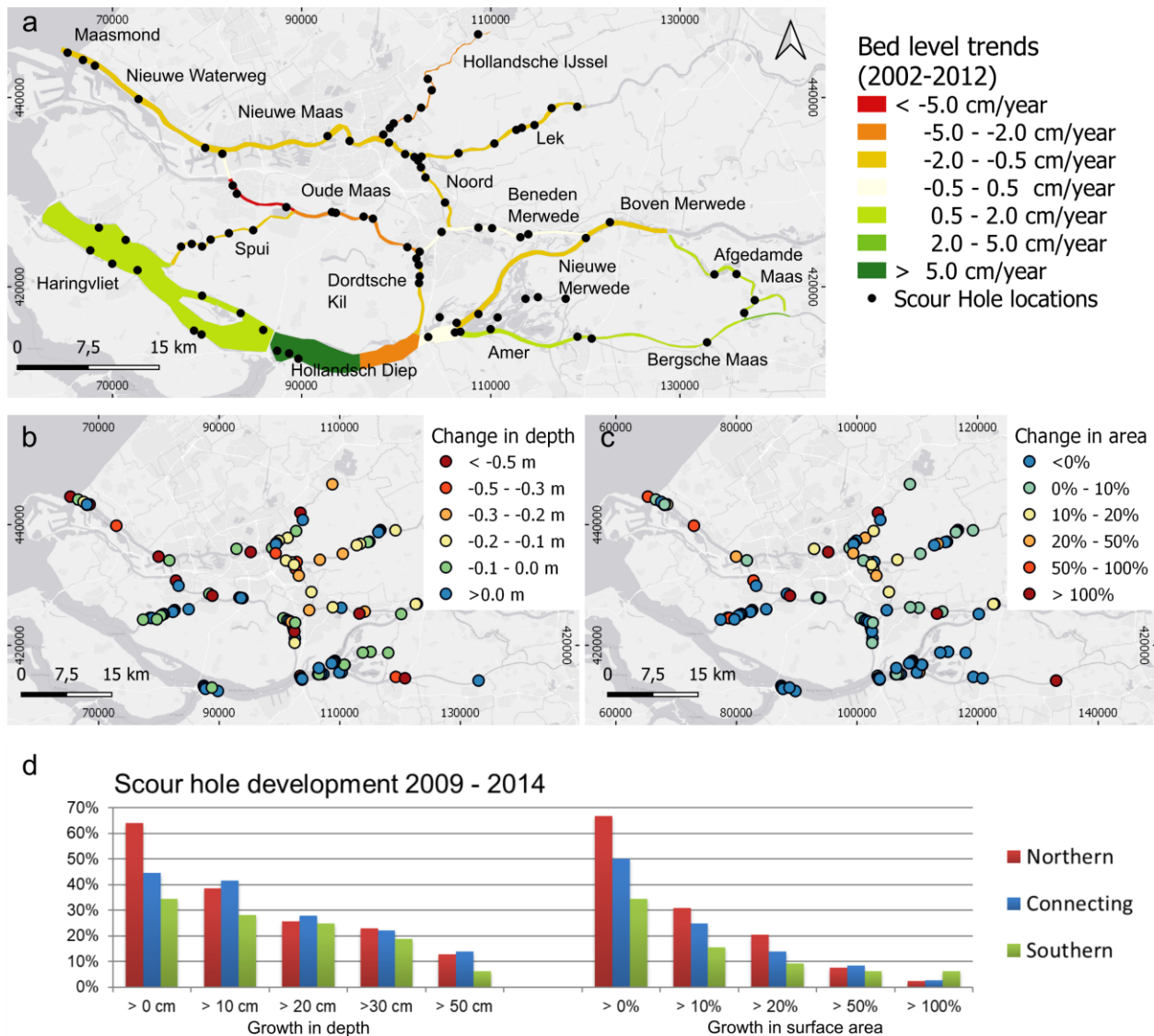
306

Figure 4 a) overview of the bed level trends 2002-2012 (data from Becker (2015)) and the identified scour holes (locations from Huismans et al., 2016) of the Rhine-Meuse Estuary. b-c) Five-year scour hole growth in depth (left) and extent (right) (this paper). d) Bar plot of the growth rates per region, namely southern branches (Merwedes, Bergsche Maas, Amer, Haringvliet, Hollandsch Diep), connecting branches (Spui, Oude Maas, Dordtsche Kil and Noord) and northern branches (Maasmond, Nieuwe Waterweg, Nieuwe Maas, Hollandsche IJssel and Lek). Maps are created in QGIS with the Esri-Grey (light) base map.

The scour holes in the southern branches (Merwede rivers, Bergsche Maas, Amer, Haringvliet, Hollandsch Diep) show the smallest growth. The strongest growth is found in the connecting (Spui,

315 Oude Maas, Dordtsche Kil and Noord) and northern channels (Maasmond, Nieuwe Waterweg,

316 Nieuwe Maas, Hollandsche IJssel and Lek). Note that without dredging, the northern branches

317 would on average show aggradation instead of degradation. This means that the strongest scour

318 hole growth is not necessarily found in the branches with the highest erosion rate.

319   4.2 Scour hole formation in the eroding branches

320   To understand how the subsurface lithology controls bed degradation and scour hole

321 development, the bed level evolution from 1976 to 2015 is studied for two eroding branches, the

322 Dordtsche Kil and Oude Maas. First, the geometric setting is introduced in Figure 5, because this

323 can influence the scour hole growth via turbulent flows induced by e.g., confluences, bends, and

324 structures. Scour holes are found in both straight and curved parts of the river, where they are

325 superimposed on a mild pool-riffle morphology (Leopold & Wolman, 1960; Leopold et al., 1964).

326 Note that most bends are mildy curved with radii greater than 2 km. Only three bends show

327 somewhat stronger curvatures with radii ranging between 1 – 1.7 km. Scour hole number 17 is

328 caused by bridge piers, while scour holes 6, 7 and 14 are located less than 500 m downstream from

329 a river confluence. This shows that a clear trigger is present for some of the scour holes. To explain

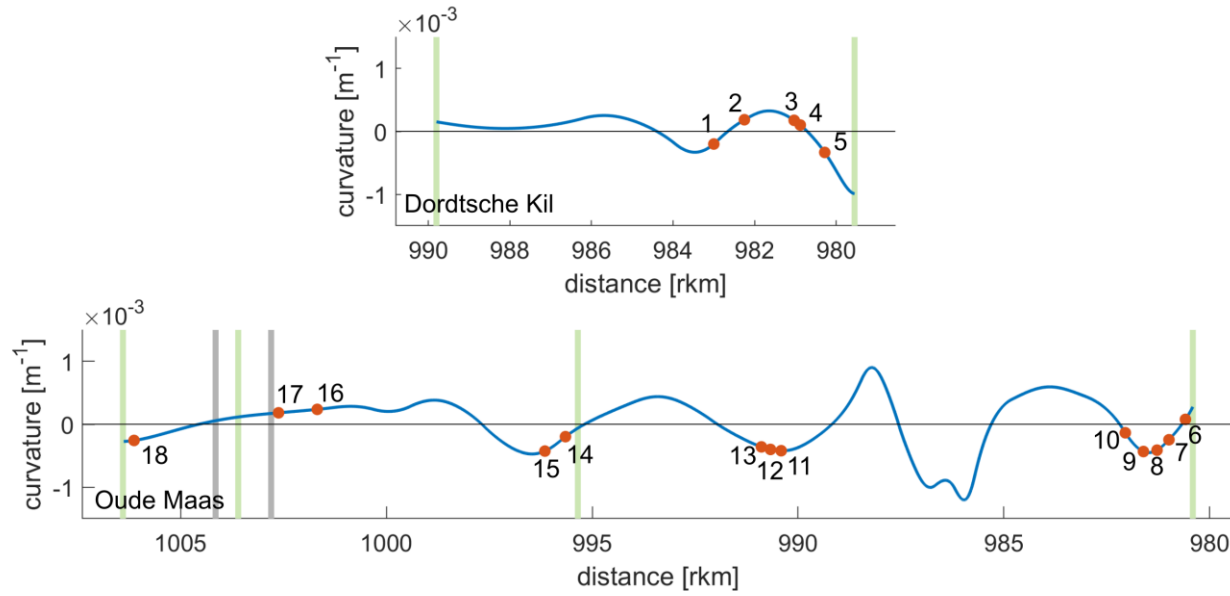330 the rest of the scour holes, we must also account for the underlying geology.

Figure 5. Inverse value of the radius of curvature plotted against the distance along the river. Red dots indicate the scour hole locations, the green bars the confluences and the grey bars the bridges. As groyne scours are excluded from the database, these are not indicated.

Figure 6 shows the development of bed elevation in time of the Dordtsche Kil. In four decades, several meters of erosion have occurred. There is a distinct difference between the northern part (between river km 980 – 983) and the southern part (river km 983 – 989) of the river. In the southern part, the river bed eroded rather homogeneously. In the northern part, the erosion is less, and spread unevenly. This coincides with the composition of the subsurface lithology, which in the southern part is homogeneous, consisting of Pleistocene sand, allowing for homogeneous erosion. The subsurface lithology in the northern part is heterogeneous and composed of resistant clay interspersed with highly erodible sand bodies from abandoned and buried channel belts. At locations where the river bed is composed of clay, erosion rates are suppressed, while in the highly erodible sand bodies, scour holes have emerged or existing scour holes have undergone further erosion. Hence, the palaeo-channel belts mapped on land on both sides of the river are clearly visible in the river morphology as scour holes.

347   A major engineering intervention that may have affected the scour hole growth is the

348   reconstruction of the Dordtsche Kil, where the navigation channel was modified and deepened to

349   -8 m NAP between 1970 – 1984 (Table 1). Figure 6a shows that most of the scour holes were

350   already present in 1976, though mostly with limited depth. It cannot be verified whether the scour

351   holes were initiated by natural erosion, or whether dredging to -8 m NAP caused a resistant layer

352   covering the channel belts to be removed, allowing for faster erosion in the channel belts than in

353   the surrounding resistant clay and peat bed. Regardless of the cause of erosion, without

354   heterogeneous subsurface lithology, no scour holes would have emerged, as there are no triggers

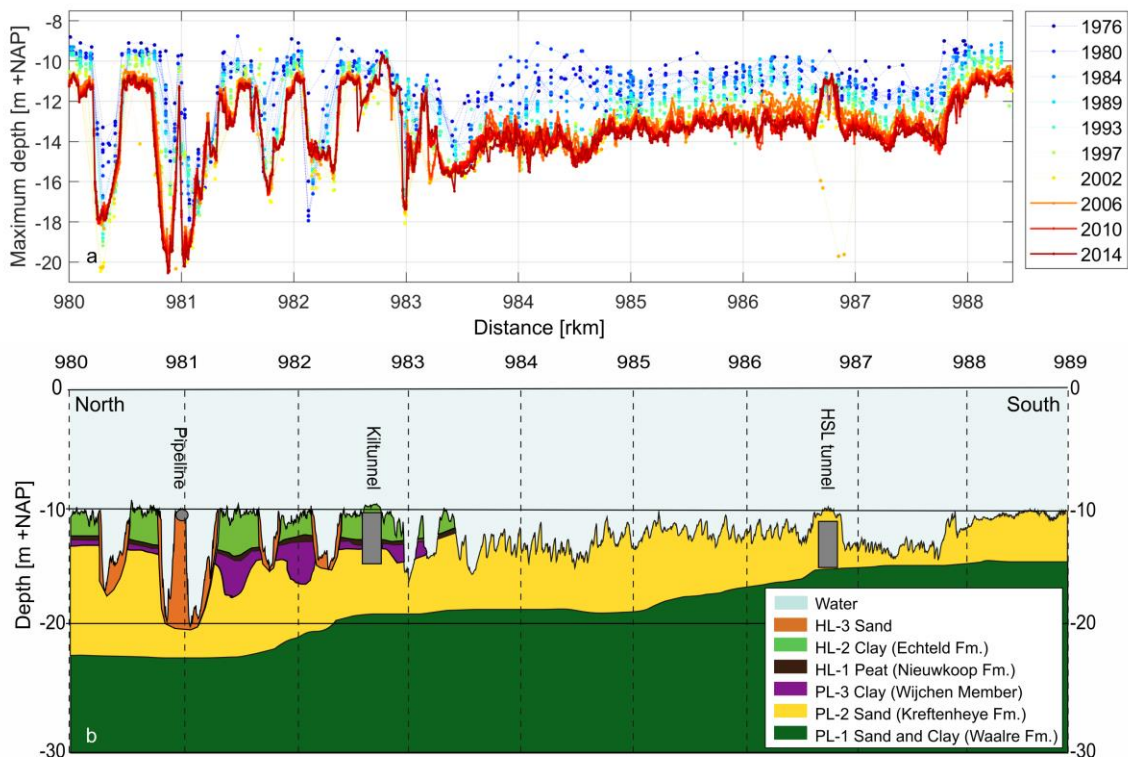355   present for causing such local scour, like constructions, sharp bends or confluences.
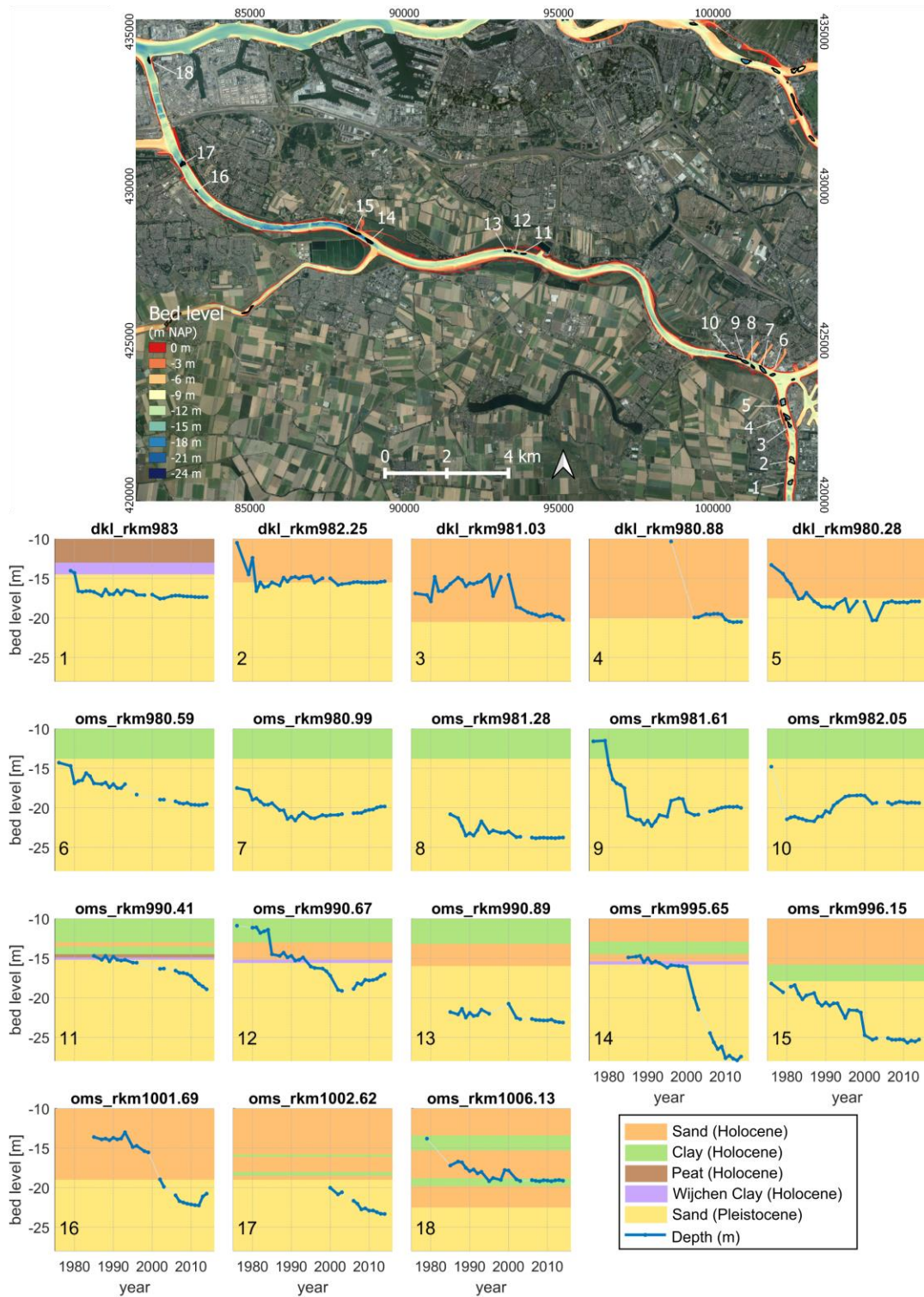
356

357   *Figure 6 a) evolution of the thalweg in the Dordtsche Kil river bed from 1976 to 2014. b) lithological longitudinal*

358   *section of the Dordtsche Kil (figure based on the report by Wiersma, 2015).*

359   For 18 scour holes in the Oude Maas and Dordtsche Kil river, we analyse the evolution of

360   the scour hole depth for the period 1976 – 2014 (Figure 7). All scour holes have been subject to

361   the same change in trend, namely an increase in flow velocities and resulting transport gradient

362   due to closure of the Haringvliet. All scour holes have consequently grown in depth. The net

363   increase in depth however strongly varies per scour hole. The largest net increase observed is 13 m,

364   which occurred in 35 years (scour hole 14, Figure 7), and the smallest net increase is approximately

365   1 m, which occurred in 29 years (scour hole 13). The depth growth rates strongly vary as well.

366   Some scour holes show a more gradual growth, whilst the growth of others is episodic. In addition,

367   the timing of acceleration or deceleration in growth is different for each scour hole. Recent rates

368   of depth change are generally lower than the overall growth rates. For 14 out of the 18 scour holes

369   the average growth rate over the last five years is less than the average growth rate over the total

370   period. Five scour holes even show net sedimentation instead of erosion over the last five years.

371   To get an indication of whether changes in growth rate can be related to the composition

372   of the subsurface lithology, the interpretation of the local subsurface lithology is presented in

373   colour in the graphs in Figure 7. For the Oude Maas the interpretation was based on limited data

374   (Stouthamer & De Haas, 2011), and at some scour hole locations no interpretation could be made

375   due to lack of data. For these scour holes, either the closest subsurface lithology is taken as an

376   indication (scour holes 6-9, 11, 14, 15 and 16, data on average available within 800 m from the

377   scour hole location), or an interpolation of the closest by subsurface lithology is taken (scour holes

378   12 and 13).

379

Figure 7 Top panel: map with scour hole locations considered for this analysis. Bed level is from 2014. Map is created

in QGIS with the Esri-Satellite base map. Bottom panel: scour hole evolution over four decades. For each scour hole

the evolution of the deepest point is shown in blue. In colour the subsurface lithology is presented.

383   The graphs show that for scour holes 1, 9, 10, 12 14, and 18, the increase in growth rate

384   corresponds with a transition to a layer with a higher erodibility and cannot be related to abrupt

385   flow changes in response to engineering interventions (Table 1). It is furthermore unlikely that

386   dredging has caused these strong variations in depth, as dredging is limited to the shallow areas.

387   For scour holes 2, 4, 5, and 18, a decrease in growth rate coincides with a transition to a layer with

388   lower erodibility. For some scour holes (11, 15, and 16), the increase in growth rate cannot directly

389   be related to changes in erodibility. For scour holes 11 and 15, the transition to faster growth

390   happens at larger depth than the transition from clay to Pleistocene sand. As no interventions are

391   known that can explain the increase in growth rate (Table 1), it is likely that the clay to sand

392   transition is locally lower than suggested by the lithological longitudinal section. For scour hole

393   16, the depth at which the growth rate increases is in the middle of a sand layer. The nearby

394   subsurface lithology is however very heterogeneous. Within 1 km a clay layer is present at -16 m

395   NAP, exactly the depth at which the growth rate increased. This gives a strong indication that the

396   transition to a faster growth is induced by a transition from clay to sand.

397   4.3 Detailed growth in relation to the subsurface lithology

398   To estimate the risk of scour holes on the stability of nearby structures and river banks,

399   predictions on the scour hole growth rate and direction are required. For this purpose, two river

400   sections with scour holes of distinct size, shape, growth rate, and direction are analysed in relation

401   to their subsurface lithology.

402   In Figure 8, the present bed level and evolution of the thalweg (1976-2015) is shown for a

403   2 km river section of the Oude Maas and Dordtsche Kil. The bed topography of the Oude Maas

404   section shows an elongated scour hole of over 1 km length and two smaller ones at river km 995.7

405   and 997.5. The evolution of the thalweg indicates that the elongated scour hole initially consisted

406   of two or three scour holes which developed in depth and extent and merged together. Both smaller

407   scour holes are not present in the 1976 surveys and only emerge around 2000 and 2005 for

408   respectively the scour hole at river km 997.5 and 995.7. The scour hole at river km 995.7 mostly

409   extends in an eastward direction but also westward, in the direction of the elongated scour hole. If

410   this trend continues, this scour hole will merge with the elongated scour hole to form an even larger
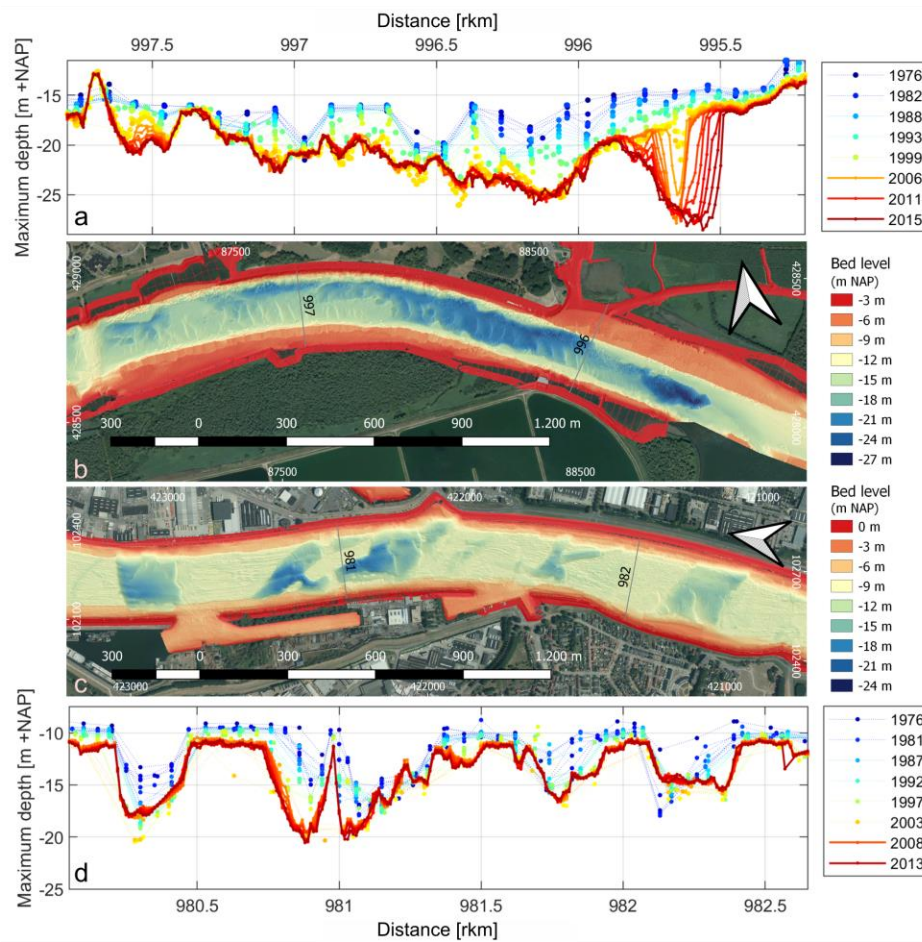
411   one.

412

413   *Figure 8 Detailed scour hole evolution for two locations. a) Evolution of the thalweg in the Oude Maas (rkm 997.25*

414   *– 995.75), b) corresponding bed topography in 2014. Residual or net sediment-transport direction is westward (to the*

415   *left in the figure). c) Bed topography Dordtsche Kil (rkm 980.1 – 982.6) in 2014 and d) corresponding evolution of*

416   *the thalweg. The residual or net sediment-transport direction is northward (to the left in the figure). Maps are created*

417   *in QGIS with the Esri-Satellite base map.*

418   The scour hole size, growth and shape observed in the displayed section of the Dordtsche

419   Kil, are very different from the scour holes in the Oude Maas section. The scour holes are smaller,

420   with a length of about 200 to 300 m and are irregularly shaped, with seemingly artificial shapes

421   containing sharp angles and rectangular features. None of the scour holes merged, nor are trends

422   observed which suggest that scour holes will merge. Over the last 8 years, the scour holes show

423   only minor evolution.

424   The bed topography east of the scour hole in the Oude Maas (rkm < 995.5, bed elevation

425   around NAP -16 m) is very smooth, suggesting the presence of a clay layer, which prevents the

426   formation of bed forms (Fig. 9). Adjacent core descriptions indicate this is likely clay from the

427   Wijchen Mb., which is found to be present at an elevation of about NAP -16 m (see also the

428   subsurface lithology at rkm 995.65 in Figure 7). In and westward of the scour hole, large blocky

429   objects are visible thatare interpreted to be blocks of clay that crumbled from the edges in response

430   to undermining of the clay layer by the force of the flow. The bed topography around the scour

431   hole in the Dordtsche Kil shows elongated grooves. Distinct grooves from past dredging activities

432   or shipping scours indicate a resistant soil type in which marks do not easily smoothen or vanish,

433   likely clay. The subsurface lithological longitudinal section (Fig. 6) supports this hypothesis.
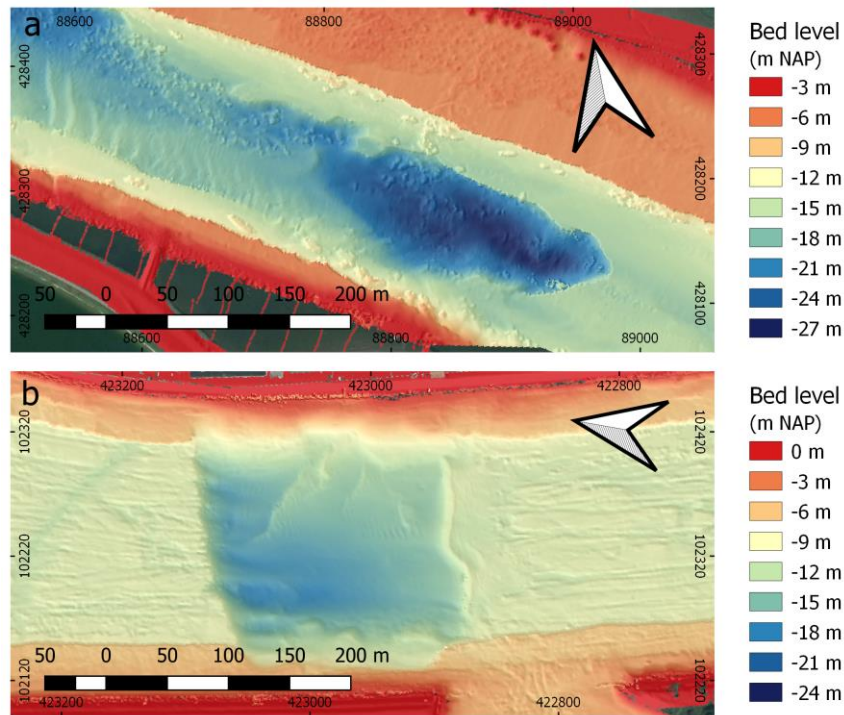
434

Figure 9 a) Bed topography of the scour hole in the Oude Maas at rkm 995.7 b) and of the scour hole in the

Dordtsche Kil at 980.2, both 2014. The smooth bed in the top figure is attributed to a clay layer. The blocks of

material in- and downstream of the scour hole are hypothesised to be blocks of clay that crumbled off the edges. The

scratches in the bottom figure are attributed to the occurrence of a resistant soil type, likely clay. They do not show

a development over time. Maps are created in QGIS with the Esri-Satellite base map.

Based on these observations, the difference in shape and opposite trends in scour hole

evolution in the displayed Oude Maas and Dordtsche Kil reach can be related to the subsurface

lithology. The scour holes in the Oude Maas are formed by abrasion of the clay layer and ultimately

breaching through this layer, such that the underlying Pleistocene sand gets exposed to the flow.

The edges of the scour holes consist of a relatively thin layer of clay (1 to 2 m), which is thin

enough to get crumbled at the edges (Fig. 9). As a result, scour holes extend both in depth and

area, and eventually merge. The Dordtsche Kil scour holes are formed in the sandy channel-belt

sand bodies that are crossed by the current river course. According to the lithological longitudinal

448   section in Figure 6, the subsurface flanking the channel-belt sand bodies consists of thick layers

449   of resistant peat and clay with a varying thickness of 3 to 8 meter, suppressing erosion in lateral

450   direction and confining the scour holes to the size of the channel belt. This may also explain the

451   typical rectangular like shape of some of the scour holes, as the current river channel crosses the

452   channel-belt sand bodies. The sharp angles in the scour contour may be related to outcrops of

453   peat/clay. Though the thick peat and clay layer currently confines the scour holes to the area of the

454   channel belt, slopes within the scour holes are observed to slowly get steeper, indicating that

455   growth has not stopped entirely.

456   To further verify whether the shape of the scour hole indeed relates to the subsurface

457   lithology, we determined the length and width of the scour holes in the Dordtsche Kil and Oude

458   Maas and related them to the composition at the scour edge (Fig. 10). The analysis confirms that

459   scour holes with edges composed of sand or a thin layer of clay are generally more elongated than

460   scour holes of which both edges are composed of a thick layer of poorly erodible material.

461   Though these observations are a strong indication of the dominant role of lithology in the

462   horizontal scour hole growth, the role of the flow remains to be verified, especially as the

463   difference between confined and elongated scour holes largely coincides with the branch in which

464   they are located. According to one dimensional flow simulations presented in Table 2, the

465   velocities in the Dordtsche Kil and Oude Maas are very comparable. The only notable difference

466   is the asymmetry in ebb and flood flow velocities, which is stronger for the Oude Maas. The

467   potential effect is a stronger erosion during ebb tidal currents than during flood tidal currents in

468   the Oude Maas, and a more equal erosion during ebb and flood tidal current in the Dordtsche Kil.

469   This can however not explain the differences in shape and horizontal growth. Scour holes of which

470   the scour hole edges are composed of sand or a thin layer of clay (all in the Oude Maas) are

observed to erode in both ebb- and flood flow direction. This suggests that both ebb and flood tidal flow velocities are strong enough to cause erosion. In the Dordtsche Kil, both the ebb and flood tidal flow velocities are comparable to the ebb current and stronger than the flood current of the Oude Maas. If the scour edges were composed of the same material as in the Oude Maas, the scour holes in the Dordtsche Kil would also erode in both directions. As the ebb flow velocities in the Dordtsche Kil exceed the ebb flow velocities in the Oude Maas, the erosion potiential in the ebb- current direction would even be stronger, causing potentially even more elongated scour holes. However, this is the opposite from what is observed. The observations of scour holes in the Dordtsche Kil show that they stay confined and barely expand in the ebb or flood flow direction; only their internal edges steepen. Therefore, we conclude that the difference in flow conditions between the Dordtsche Kil and Oude Maas cannot explain the differences in confined versus more elongated expanding scour holes. This further strengthens the evidence that the lithology causes the observed differences.

Figure 10. Length-width ratios of the scour holes from the Dordtsche Kil and Oude Maas. In color the composition and thickness of the scour hole edge is displayed, where "cb" indicates a scour hole formed in a channel belt and "wm" indicates that the scour hole edges are composed of clay from the Wijchen Mb. A separate class is made for the bridge pier scour, as these are scour holes formed around two bridge piers and the surrounding bed is (partially) stabilised with Riprap.

490

5 Discussion

5.1 Lithological control on scour hole formation

Most prominent from the analysis is the diversity of the size, shape, and growth characteristics of the scour holes. Various factors likely contribute. Firstly, the causes that trigger scour hole formation include turbulent flows induced by river bends (e.g., Engelund, 1974; Zimmermann & Kennedy, 1978; Odgaard, 1981; Andrle, 1994; Gharabaghi et al., 2007; Blanckaert, 2010; Beltaos et al., 2011; Ottevanger et al., 2012; Vermeulen et al., 2015), confluences (e.g., Mosley, 1976; Kjerfve et al., 1979; Best, 1986; Ginsberg & Perillo, 1999; Pierini et al., 2005; Best & Rhoads, 2008Ginsberg et al., 2009; Ferrarin et al., 2018), local channel narrowings and structures, like bridge piers, groynes and bed protection (e.g., Wang et al., 2017; Pandey et al., 2018; Liang et al., 2020). These types of scour holes evolve differently, have different shapes, and as a result have different relations for predicting their equilibrium depth (Hoffmans & Verheij, 1997). As illustrated in Figure 5, some of the scour holes are indeed triggered by such turbulent flows. Secondly, conditions that influence scour hole growth like flow velocity, water depth, and grain size vary throughout the estuary. The third reason is the lithological influence on scour hole formation, which in current analyses proves to be a major influence on scour hole initiation, growth rate, and shape, and which in certain cases even overrules the above causes and controls. In Figure 11, the three lithological controls are illustrated conceptually. Firstly, lithology may trigger scour hole formation (Fig. 11a). A prominent example is the large-scale incision of the Dordtsche Kil river into the heterogeneous subsurface lithology, leading to formation of scour holes of up to two times the average water depth at locations where the erosion resistant peat and clay layers are interrupted by channel belt sand bodies. Though it

513 cannot be determined whether the protecting top layer covering the sand bodies was removed by

514 natural erosion or by deepening the Dordtsche Kil to -8 m NAP (1970-1984), in both cases the

515 heterogeneous subsurface lithology is the only explanation for the presence of scour holes. Without

516 the heterogenous subsurface lithology, the river branch would have dropped evenly in response to

517 natural erosion or deepening, as happened in the southern part. This forms the most direct proof

518 that variations in lithology cause scour hole formation. It is in line with observations by Cserkész-

519 Nagy et al. (2010), who reasoned that scour holes observed in a straight river section were triggered

520 by variations in the subsurface lithology, and with Sloff et al. (2013) who demonstrated this

521 process conceptually and numerically.

522 Secondly, lithology determines whether and when a scour hole can form and when

523 fluctuations in growth rate occur (Fig. 11b). An insightful example is the scour hole at the

524 confluence of the Spui and Oude Maas river (Figs. 7-8). Though the confluence in its present

525 outline has already existed for over a century as visible in historical maps (www.topotijdreis.nl),

526 no confluence scour emerged until recently, in 2005. Only after reaching a transition from resistant

527 clay to sand, in ten years' time a scour hole with a depth of -27 m NAP emerged, i.e., an average

528 growth in depth of 11 m in 10 year. These abrupt changes in growth in depth are observed for

529 various scour holes in the Rhine-Meuse Estuary (Fig. 7) and can in most cases be related to a

530 transition in lithology with different erodibility. Though not proven, it is also the most likely cause

531 for abrupt changes in growth for the other scour holes, as other causes such as a strong increase in

532 flow, new constructions, dredging or failure of bed protection do not apply.

I. Initiation: Scour hole or no scour hole

Legend:
- Water
- Sand
- Clay/peat
- Sand (channel belt)
- Construction
- --- Bed evolution

Case No hydrodynamic trigger for local scour
Homogeneous (no scour hole) vs. heterogeneous subsurface (scour hole)

II. Growth: acceleration and deceleration

Bridge pier

depth / time

Case Hydrodynamic trigger for local scour, e.g. structure, confluence, bend, ...
Homogeneous (smooth grow) vs. heterogeneous subsurface (irregular growth)

III. Shape: confined & steep slopes vs. expanding & milder slopes

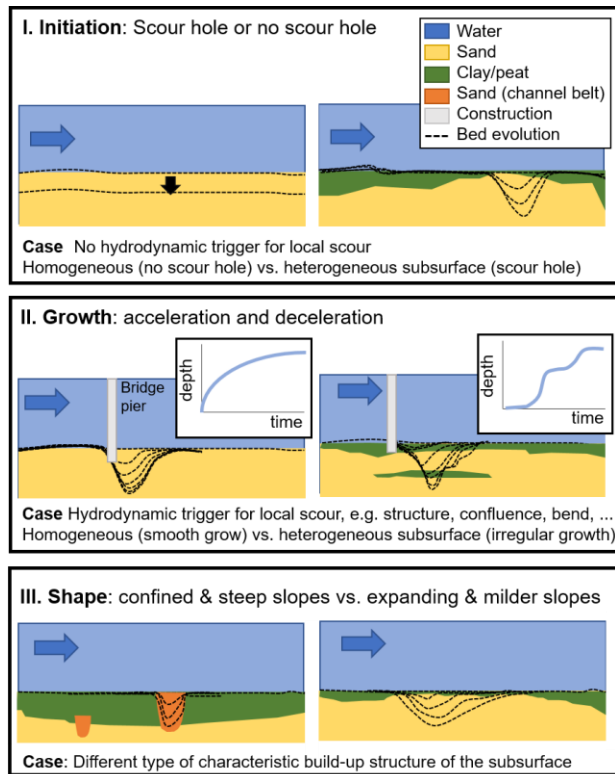**Case**: Different type of characteristic build-up structure of the subsurface

Figure 11. Summary of the observed lithological controls on scour hole development. All figures display a longitudinal section of a river reach, with the blue arrow indicating the flow direction. Dashed lines represent the bed level development over time.

Thirdly, in horizontal direction the subsurface lithology can be a dominant factor in determining the shape or growth rate (Fig. 11c). Scour holes with edges composed of thin layers of clay (< 2 m thickness), are observed to grow in extent. In high resolution multibeam surveys, indications are found that these clay layers are undermined and crumble, enabling the scour hole to grow laterally and merge with nearby scour holes. As a result, scour holes of more than a kilometre in length form. The opposite is observed for the scour holes in the Dortdsche Kil, which are relatively small (< 300 m in length) and show only subtle changes in horizontal direction. These scour holes are formed in former channel belts sand bodies and their edges consist of thick layers of peat and clay (3 to 8 m thickness), confining the scour holes to the extent of the channel belt, suppressing further growth in extent.

547   The strong lithological control on scour hole formation is in line with the reported effect

548   of the subsurface lithology on the formation of ebb-tidal channels in the Ems (Pierik et al., 2019)

549   and erosion and lateral migration of the Tisza river (Cserkész-Nagy et al., 2010). It may also

550   explain the deviations in expected scour depth, location and shape observed in the Venice Lagoon

551   (Ferrarin et al., 2018).

552

553   5.2 Equilibrium

554   There is no clear relation between recent five-year scour hole growth and overall bed level

555   degradation. This means that the strongest scour hole growth is not necessarily found in the

556   branches with the highest erosion rate. The occurrence of local scour and sand mining may explain

557   some of these cases, but a closer look at the 40-year depth evolution of the scour holes in the

558   eroding Dordtsche Kil and Oude Maas branches shows that for most of the scour holes, the recent

559   depth growth rates have decreased or even reversed to sedimentation. In response to the higher

560   flow velocities due to closure of the Haringvliet, the scour hole depth increased for all cases. As

561   Haringvliet was closed decades ago, it is likely that most scour holes are reaching an equilibrium

562   depth, like also occurs for local scour induced by constructions (Hoffmans & Verheij, 1997). That

563   an equilibrium depth also applies for the scour holes induced or influenced by a heterogeneous

564   subsurface lithology is plausible, as the same physics apply. The deeper the scour hole gets, the

565   more energy it takes to transport sediment up the slope, while depending on how the flow structures

566   evolve, generally the flow velocities within the scour hole decrease with depth. Another

567   explanation for a slower or reversed depth development may be the presence of an erosion resistant

568   layer at the bottom of the scour hole (Cserkész-Nagy et al., 2010). This is clearly the case for scour

569   hole 18 (Fig. 7), which reached a resistant clay layer. It may also be a factor for the scour holes in

570   the Dordtsche Kil, as the depth of the channel-belt sand bodies in which the scour holes formed is

571   interpreted to be close to the current scour hole depth (Fig. 6). As the channel-belt bodies are

572   commonly composed of finer grained sands than the coarser grained Pleistocene sand layer below

573   (e.g. Berendsen, 1982; Weerts & Busschers, 2003; Gouw & Erkens, 2007), the erodibility is lower,

574   reducing the scour hole depth growth. According to the lithological longitudinal sections, most of

575   the Oude Maas scour holes are already based within the Pleistocene sand and are not at a depth

576   close to reaching a transition in lithological composition. However, as the Pleistocene sand

577   gradually coarsens with depth (Busschers et al., 2005, 2007), this may still have an impact. For

578   these scour holes, it is likely that a combination of coarsening of sediment with reduced hydraulic

579   forcing due to reaching a larger depth results in a reduced growth or stabilization of depth. To

580   further quantify the relative contributions of each process, a combination of flow measurements

581   and calculations with data on the grain size distribution in the lower part of the scour hole is

582   needed.

583   5.3 Consequences and risks for other rivers and estuaries

584   Provided sufficiently strong hydraulic forcing, the subsurface lithology can have a large

585   impact on when and where scour holes form, or even be dominant. The observed influences and

586   controls on initiation, growth rates and size, as illustrated in Figure 11, apply to any system with a

587   heterogeneous substratum of alternating peat, clay and sand deposits. Though little has been

588   reported, these controls are likely not unique to the Rhine-Meuse Estuary. Channel bed degradation

589   by natural erosion or channel deepening, also happens in other large delta rivers like the Yangtze,

590   the Mississippi and the Mekong (Galler et al., 2003; Sloff et al., 2013; Brunier et al., 2014; Luan

591   et al., 2016; Hoitink et al., 2017; Wang & Xu, 2018). And as causes are mainly anthropogenic,

592   more delta rivers are expected to follow. Because river deltas commonly have a heterogeneous

593 substratum of alternating peat, clay and sand deposits (e.g. Aslan & Autin, 1999; Berendsen &

594 Stouthamer, 2001, 2002; Aslan et al., 2005; Kuehl et al., 2005; Stefani & Vincenzi, 2005; Gouw

595 & Autin, 2008; Cohen et al., 2012; Hanebuth et al., 2012), scour hole formation in heterogeneous

596 subsurface is expected to become a problem in more deltas. Data suggest that for the Ems river

597 (Pierik et al. 2019), the Venice Lagoon (Ferrarin et al., 2018), lower Mississippi River (Nittrouer

598 et al., 2011) and the Mekong River, the subsurface lithology already plays a role in the scour hole

599 development, as scour holes in these studies show deviating location, shape or depth, while the

600 subsurface is heterogeneous. When for these systems only the hydraulic component is taken into

601 account, as commonly the case, there will be a misprediction of the scour hole evolution, depth,

602 shape and location. In case where scour holes are close to infrastructure or river banks, stability is

603 at stake. Also, in case of channel deepening, it is important to know the subsurface lithology. In

604 case a resistant clay or peat layer gets removed, sudden scour hole formation can occur in response

605 to deepening, as potentially happened in de Dordtsche Kil. As accurate predictions of scour hole

606 formation are highly important, especially in densely occupied areas like deltas (Syvitski et al.,

607 2009; Best, 2019), we advocate to explicitly consider the underlying geology when predicting

608 scour hole formation and growth. This requires knowledge of the subsurface lithology, acquired

609 via a combination of measurements and geological interpretation, as elaborated in the methods

610 section. Based on the specific geological structure, the risk of new scour hole formation can be

611 assessed, as well as the likelihood whether scour holes stay confined or expand. Given the other

612 controls of lithology on the depth of meander pools (Hudson, 2002; Gibson et al., 2019), the lateral

613 behaviour of river branches (Cserkész-Nagy et al., 2010) and the evolution of ebb-flood channels

614 (Pierik et al., 2019), it is important to include the lithology into numerical models (van der Wegen

615 & Roelvink, 2012). Therefore, measuring subsurface lithology and including these parameters in

616   scour-hole risk-assessments and numerical models will be an important improvement over current

617   analyses, which focus mainly on the hydraulic forcing assuming a homogenous substrate.

618   **6 Conclusions**

619   Although a vast amount of research has been carried out on scour holes, little is known on

620   how the lithology influences the location, size, shape and growth rates of scour holes. This is,

621   however, essential information in judging whether scour holes form a risk for the stability of river

622   banks, dikes or other nearby infrastructure. The present study presents a first in depth analysis on

623   how the lithology controls the bed topography and scour hole growth in particular. The Rhine-

624   Meuse estuary is used as a study area, as over 100 scour holes are present and detailed data are

625   available on both bed level evolution and subsurface lithological composition.

626   From analysing over 40 years of bed level evolution in relation to the geology, it is shown

627   that subsurface lithology can play a crucial role in the emergence of scour holes, their shape and

628   evolution. In the Rhine-Meuse Estuary several branches are eroding in response to closure of one

629   of its tidal outlets. Reaches with a sandy subsurface erode evenly, while in reaches with a

630   heterogeneous subsurface lithology, erosion is retarded at locations with an erosion resistant top

631   layer and promoted at locations where sand bodies are present in the subsurface. At these locations,

632   deep scour holes form with depths of up to two times the average water depth. Their shapes can

633   be very irregular and strongly deviating from classical oval shapes. These shapes are imposed by

634   the erosion resistant top layer, inhibiting the scour hole to grow more naturally in width or length.

635   The consequent growth characteristics are often erratic, with sudden changes in depth or extent.

636   Naturally, scour holes follow an exponential development with a fast initial growth and slower

637   final growth. Though this analysis shows that scour holes in heterogeneous subsurface generally

638   follow the same growth curve, temporally strong variations in development in depth or extent are

639   observed.

640   The direction of growth is also strongly determined by the composition of the subsurface.

641   Scour holes with edges composed of thin layers of clay are observed to grow in extent. Indications

642   are found that the thin clay layers crumble and enable scour holes to grow laterally and merge with

643   nearby scour holes, forming elongated scour holes of more than a kilometre in length. The opposite

644   is observed for scour holes that are formed in channel belts with thick peat and clay layers at their

645   edges, confining the scour holes to the extent of the channel-belt sand body crossed by the river

646   channel and limiting growth in horizontal direction.

647   These findings emphasize the crucial role that geology plays in the spatial and temporal

648   evolution of river bed erosion. It co-determines the pace of erosion and the related long-term

649   evolution of river branches and tidal channels and it can initiate and influence scour hole formation.

650   It therefore calls for good knowledge of the subsurface lithology as without, the erratic scour hole

651   development is hard to predict and can lead to sudden failures of nearby infrastructure and flood

652   defence works. In addition, for making proper morphodynamic predictions, information on the

653   subsurface lithology needs to be included in numerical models.

654   **Data Availability Statement**

655   There is no restriction on the data used in this study. Bed topography data can be requested at

656   Rijkswaterstaat   via   https://www.rijkswaterstaat.nl/formulieren/contactformulier-servicedesk-

657   data.aspx. Lithological core descriptions can be downloaded from the DINO loket:

658   www.dinoloket.nl. Lithological cross-sections and longitudinal sections constructed from the

659   lithological core descriptions are available in (Huismans et. al., 2013; Stouthamer & De Haas,

660 2011; Stouthamer et al., 2011b-d; Wiersma, 2015). Channel belt reconstruction can be downloaded

661 from http://dx.doi.org/10.17026/dans-x7g-sjtw (Cohen et al., 2012). The scour hole database is

662 made available via Mendeley Data.

669

References

671 Andrle, R. (1994). Flow structure and development of circular meander pools. Geomorphology, 9(4), 261–270.

672   https://doi.org/10.1016/0169-555X(94)90049-3

673 Aslan, A., & Autin, W. J. (1999). Evolution of the Holocene Mississippi River floodplain, Ferriday, Louisiana;

674   insights on the origin of fine-grained floodplains. Journal of Sedimentary Research, 69(4), 800–815.

675   https://doi.org/10.2110/jsr.69.800

676 Aslan, A., Autin, W. J., & Blum, M. D. (2005). Causes of River Avulsion: Insights from the Late Holocene

677   Avulsion History of the Mississippi River, U.S.A. Journal of Sedimentary Research, 75(4), 650–664.

678   https://doi.org/10.2110/jsr.2005.053

679 Becker, A. (2015). Sediment in (be)weging, deel 2 (periode 2000-2012). English: Sediment budget of the Rhine

680   Meuse Estuary (2000-2012) (No. 1208925-000-ZWS-0023). Delft, the Netherlands: Deltares.

681 Beltaos, S., Carter, T., & Prowse, T. (2011). Morphology and genesis of deep scour holes in the Mackenzie Delta.

682   Canadian Journal of Civil Engineering, 38(6), 638–649. https://doi.org/10.1139/l11-034

683   Berendsen, Henk J.A, & Stouthamer, E. (2000). Late Weichselian and Holocene palaeogeography of the Rhine–

684   Meuse delta, The Netherlands. Palaeogeography, Palaeoclimatology, Palaeoecology, 161(3), 311–335.

685   https://doi.org/10.1016/S0031-0182(00)00073-0

686   Berendsen, H.J.A. (1982). De genese van het landschap in het zuiden van de provincie Utrecht, een fysisch-

687   geografische studie. (PhD-thesis). Utrecht University, Utrecht, the Netherlands.

688   Berendsen, H.J.A., Hoek, W. Z., & Schorn, E. A. (1995). Late Weichselian and Holocene river channel changes of

689   the rivers Rhine and Meuse in the central Netherlands (Land van Maas en Waal). In European river activity

690   and climate change during the Lateglacial and Early Holocene. ESF Project European Paläoklimaforschung

691   / Paleoclimate Research, Special Issue (pp. 151–171). Frenzel, B. (ed.).

692   Berendsen, H.J.A., & Stouthamer, E. (2001). Paleogeographic development of the Rhine-Meuse delta, The

693   Netherlands (1st printing). Assen: Koninklijke Van Gorcum.

694   Berendsen, H.J.A., & Stouthamer, E. (2002). Paleogeographic evolution and avulsion history of the Holocene

695   Rhine-Meuse delta, The Netherlands. Netherlands Journal of Geosciences - Geologie En Mijnbouw, 81(1),

696   97–112. Cambridge Core. https://doi.org/10.1017/S0016774600020606

697   Best, J. L. (1986). The morphology of river channel confluences. Progress in Physical Geography: Earth and

698   Environment, 10(2), 157–174. https://doi.org/10.1177/030913338601000201

699   Best, J. L., & Rhoads, B. L. (2008). Sediment transport, bed morphology and the sedimentology of river channel

700   confluences. In River confluences, tributaries and the fluvial network (pp. 45–72). Chichester, UK: In S. P.

701   Rice, A. G. Roy, & B. L. Rhoads (Eds.) John Wiley & Sons, Ltd.

702   Blanckaert, K. (2010). Topographic steering, flow recirculation, velocity redistribution, and bed topography in sharp

703   meander bends. Water Resources Research, 46(9). https://doi.org/10.1029/2009WR008303

704   Brunier, G., Anthony, E. J., Goichot, M., Provansal, M., & Dussouillez, P. (2014). Recent morphological changes in

705   the Mekong and Bassac river channels, Mekong delta: The marked impact of river-bed mining and

706   implications for delta destabilisation. Geomorphology, 224, 177–191.

707   https://doi.org/10.1016/j.geomorph.2014.07.009

708   Busschers, F. S., Kasse, C., van Balen, R. T., Vandenberghe, J., Cohen, K. M., Weerts, H. J. T., … Bunnik, F. P. M.

709   (2007). Late Pleistocene evolution of the Rhine-Meuse system in the southern North Sea basin: Imprints of

710   climate change, sea-level oscillation and glacio-isostacy. Quaternary Science Reviews, 26(25), 3216–3248.

711   https://doi.org/10.1016/j.quascirev.2007.07.013

712 Busschers, F. S., Weerts, H. J. T., Wallinga, J., Cleveringa-a2, P., Kasse, C., de Wolf, H., & Cohen, K. M. (2005).

713   Sedimentary architecture and optical dating of Middle and Late Pleistocene Rhine-Meuse deposits—Fluvial

714   response to climate change, sea-level fluctuation and glaciation. Netherlands Journal of Geosciences -

715   Geologie En Mijnbouw, 84(1), 25–41. Cambridge Core. https://doi.org/10.1017/S0016774600022885

716 Cohen, K. M. (2003). Differential subsidence within a coastal prism: Late-Glacial—Holocene tectonics In The

717   Rhine-Meuse delta, the Netherlands (PhD-thesis). Utrecht University.

718 Cohen, K. M., Stouthamer, E., Pierik, H. J., & Geurts, A. H. (2012). Digital Basemap for Delta Evolution and

719   Palaeogeography. Utrecht University. DANS. Retrieved from http://dx.doi.org/10.17026/dans-x7g-sjtw

720 Cox, J. R., Huismans, Y., Leuven, J. R. F. W., Vellinga, N. E., van der Vegt, M., Hoitink, A. J. F., & Kleinhans, M.

721   G. (submitted). Anthropogenic effects on the contemporary sediment budget of the lower Rhine-Meuse

722   Delta channel network. Preprint in ESSOAr. https://doi.org/10.1002/essoar.10506550.1

723 Cserkész-Nagy, Á., Tóth, T., Vajk, Ö., & Sztanó, O. (2010). Erosional scours and meander development in response

724   to river engineering: Middle Tisza region, Hungary. Fluvial Records as Archives of Human Activity and

725   Environmental Change, 121(2), 238–247. https://doi.org/10.1016/j.pgeola.2009.12.002

726 De Haas, T., Pierik, H. J., van der Spek, A. J. F., Cohen, K. M., van Maanen, B., & Kleinhans, M. G. (2018).

727   Holocene evolution of tidal systems in The Netherlands: Effects of rivers, coastal boundary conditions,

728   eco-engineering species, inherited relief and human interference. Earth-Science Reviews, 177, 139–163.

729   https://doi.org/10.1016/j.earscirev.2017.10.006

730 De Haas, Tjalling, van der Valk, L., Cohen, K. M., Pierik, H. J., Weisscher, S. A. H., Hijma, M. P., … Kleinhans,

731   M. G. (2019). Long-term evolution of the Old Rhine estuary: Unravelling effects of changing boundary

732   conditions and inherited landscape. The Depositional Record, 5(1), 84–108.

733   https://doi.org/10.1002/dep2.56

734 Engelund, F. (1974). Flow and bed topography in channel bends. J. Hydraul. Div., 100, 1631–1648.

735 Erkens, G. (2009). Sediment dynamics in the Rhine catchment—Quantification of fluvial response to climate change

736   and human impact. Utrecht University, Utrecht, the Netherlands.

737 Ferrarin, C., Madricardo, F., Rizzetto, F., Kiver, W. M., Bellafiore, D., Umgiesser, G., … Trincardi, F. (2018).

738   Geomorphology of Scour Holes at Tidal Channel Confluences. Journal of Geophysical Research: Earth

739   Surface, 123(6), 1386–1406. https://doi.org/10.1029/2017JF004489

740 Frings, R. M., Hillebrand, G., Gehres, N., Banhold, K., Schriever, S., & Hoffmann, T. (2019). From source to

741   mouth: Basin-scale morphodynamics of the Rhine River. Earth-Science Reviews, 196, 102830.

742   https://doi.org/10.1016/j.earscirev.2019.04.002

743 Fugro. (2002). Laboratoriumresultaten betreffende morfologisch modelleren (datarapport) (No. Opdracht-nummer

744   H-4086).

745 Galler, J. J., Bianchi, T. S., Alison, M. A., Wysocki, L. A., & Campanella, R. (2003). Biogeochemical implications

746   of levee confinement in the lowermost Mississippi River. Eos, Transactions American Geophysical Union,

747   84(44), 469–476. https://doi.org/10.1029/2003EO440001

748 Gharabaghi, B., Inkratas, C., Beltaos, S., & Krishnappan, B. (2007). Modelling of three-dimensional flow velocities

749   in a deep hole in the East Channel of the Mackenzie Delta, Northwest Territories. Canadian Journal of Civil

750   Engineering, 34(10), 1312–1323. https://doi.org/10.1139/l07-054

751 Gibson, S., Osorio, A., Creech, C., Amorim, R., Dircksen, M., Dahl, T., & Koohafkan, M. (2019). Two pool-to-pool

752   spacing periods on large sand-bed rivers: Mega-pools on the Madeira and Mississippi. Geomorphology,

753   328, 196–210. https://doi.org/10.1016/j.geomorph.2018.12.021

754 Ginsberg, S. S., & Perillo, G. M. E. (1999). Deep-scour holes at tidal channel junctions, Bahia Blanca Estuary,

755   Argentina. Marine Geology, 160(1), 171–182. https://doi.org/10.1016/S0025-3227(99)00019-5

756 Gouw, Marc J.P., & Autin, W. J. (2008). Alluvial architecture of the Holocene Lower Mississippi Valley (U.S.A.)

757   and a comparison with the Rhine–Meuse delta (The Netherlands). Sedimentary Geology, 204(3), 106–121.

758   https://doi.org/10.1016/j.sedgeo.2008.01.003

759 Gouw, M.J.P., & Erkens, G. (2007). Architecture of the Holocene Rhine-Meuse delta (the Netherlands)—A result of

760   changing external controls. Netherlands Journal of Geosciences - Geologie En Mijnbouw, 86(1), 23–54.

761   Cambridge Core. https://doi.org/10.1017/S0016774600021302

762 Hanebuth, T. J. J., Proske, U., Saito, Y., Nguyen, V. L., & Ta, T. K. O. (2012). Early growth stage of a large delta—

763   Transformation from estuarine-platform to deltaic-progradational conditions (the northeastern Mekong

764   River Delta, Vietnam). Sedimentary Geology, 261–262, 108–119.

765   https://doi.org/10.1016/j.sedgeo.2012.03.014

766   Hijma, M. P. (2009). From river valley to estuary. The early-mid Holocene transgression of the Rhine-Meuse valley,

767   The Netherlands. (PhD-thesis). KNAG/Faculty of Geographical Sciences, Utrecht University, Utrecht.

768   Hijma, M. P., & Cohen, K. M. (2011). Holocene transgression of the Rhine river mouth area, The

769   Netherlands/Southern North Sea: Palaeogeography and sequence stratigraphy. Sedimentology, 58(6),

770   1453–1485. https://doi.org/10.1111/j.1365-3091.2010.01222.x

771   Hijma, M. P., Cohen, K. M., Hoffmann, G., Van der Spek, A. J. F., & Stouthamer, E. (2009). From river valley to

772   estuary: The evolution of the Rhine mouth in the early to middle Holocene (western Netherlands, Rhine-

773   Meuse delta). Netherlands Journal of Geosciences - Geologie En Mijnbouw, 88(1), 13–53. Cambridge

774   Core. https://doi.org/10.1017/S0016774600000986

775   Hoffmans, G. J. C. M., & Verheij, H. J. (1997). Scour Manual. Rotterdam: A.A.Balkema.

776   Hoitink, A. J. F., Wang, Z. B., Vermeulen, B., Huismans, Y., & Kästner, K. (2017). Tidal controls on river delta

777   morphology. Nature Geoscience, 10, 637.

778   Hudson, P. F. (2002). Pool-Riffle Morphology in an Actively Migrating Alluvial Channel: The Lower Mississippi

779   River. Physical Geography, 23(2), 154–169. https://doi.org/10.2747/0272-3646.23.2.154

780   Huismans, Y., van Velzen, G., O'Mahony, T. S. D., Hoffmans, G. J. C. M., & Wiersma, A. P. (2016). Scour hole

781   development in river beds with mixed sand-clay-peat stratigraphy. ICSE Conference 2016, Oxford UK.

782   Huismans, Y., Wiersma, A., Blinde, J., van Kesteren, W., & Mosselman, E. (2013). Erosie door het verwijderen van

783   boomstammen uit de Merwedes (Definitief No. 1206826-000-ZWS-0020). Deltares.

784   Janssens, M. M., Kasse, C., Bohncke, S. J. P., Greaves, H., K.M. Cohen, undefined, Wallinga, J., & Hoek, W. Z.

785   (2012). Climate-driven fluvial development and valley abandonment at the last glacial-interglacial

786   transition (Oude IJssel-Rhine, Germany). Netherlands Journal of Geosciences - Geologie En Mijnbouw,

787   91(1–2), 37–62. Cambridge Core. https://doi.org/10.1017/S001677460000055X

788   Kjerfve, B., Shao, C.-C., & Stapor, F. W. (1979). Formation of deep scour holes at the junction of tidal creeks: An

789   hypothesis. Marine Geology, 33(1), M9–M14. https://doi.org/10.1016/0025-3227(79)90126-9

790   Kuehl, S. A., Allison, M. A., Goodbred, S. L., & Kudrass, H. (2005). The Ganges-Brahmaputra Delta. In: Giosan, L.

791   & J.P. Bhattacharya (Eds.). In River deltas—Concepts, Models and Examples. SEPM Special Publication

792   83.

793   Leopold, L. B., & Wolman, M. G. (1960). River meanders. Geological Society of America Bulletin, 71(6), 769–793.

794   USGS Publications Warehouse. https://doi.org/10.1130/0016-7606(1960)71[769:RM]2.0.CO;2

795   Leopold, L. B., Wolman, M. G., & Miller, J. P. (1964). Fluvial processes in geomorphology. New York, NY: Dover

796   Publications, Inc. USGS Publications Warehouse. Retrieved from

797   http://pubs.er.usgs.gov/publication/70185663

798   Liang, B., Du, S., Pan, X., & Zhang, L. (2020). Local Scour for Vertical Piles in Steady Currents: Review of

799   Mechanisms, Influencing Factors and Empirical Equations. J. Mar. Sci. Eng., 8(4).

800   https://doi.org/10.3390/jmse8010004

801   Luan, H. L., Ding, P. X., Wang, Z. B., Ge, J. Z., & Yang, S. L. (2016). Decadal morphological evolution of the

802   Yangtze Estuary in response to river input changes and estuarine engineering projects. Geomorphology,

803   265, 12–23. https://doi.org/10.1016/j.geomorph.2016.04.022

804   Madricardo, F., Foglini, F., Campiani, E., Grande, V., Catenacci, E., Petrizzo, A., … Trincardi, F. (2019). Assessing

805   the human footprint on the sea-floor of coastal systems: The case of the Venice Lagoon, Italy. Scientific

806   Reports, 9(1), 6615. https://doi.org/10.1038/s41598-019-43027-7

807   Mosley, M. P. (1976). An Experimental Study of Channel Confluences. The Journal of Geology, 84(5), 535–562.

808   https://doi.org/10.1086/628230

809   Nittrouer, J. A., Mohrig, D., Allison, M. A., & Peyret, A. P. B. (2011). The lowermost Mississippi River: A mixed

810   bedrock-alluvial channel. Sedimentology, 58(7), 1914–1934. https://doi.org/10.1111/j.1365-

811   3091.2011.01245.x

812   Odgaard, A. J. (1981). Transverse Bed Slope in Alluvial Channel Bends. J. Hydraul. Div., 107(12), 1677–1694.

813   Ottevanger, W., Blanckaert, K., & Uijttewaal, W. S. J. (2012). Processes governing the flow redistribution in sharp

814   river bends. Meandering Channels, 163–164, 45–55. https://doi.org/10.1016/j.geomorph.2011.04.049

815   Pandey, M., Ahmad, Z., & Sharma, P. K. (2018). Scour around impermeable spur dikes: A review. ISH Journal of

816   Hydraulic Engineering, 24(1), 25–44. https://doi.org/10.1080/09715010.2017.1342571

817   Pierik, H. J., Busschers, B., & Kleinhans, M. G. (2019). De rol van resistente lagen in de historische morfologische

818   ontwikkeling van het Eems-Dollard estuarium vanaf de 19e eeuw. Utrecht, the Netherlands: Universiteit

819   Utrecht, Faculteit Geowetenschappen, Departement Fysische Geografie and TNO Geologische Dienst

820   Nederland, Utrecht.

821   Pierik, H. J., Stouthamer, E., Schuring, T., & Cohen, K. M. (2018). Human-caused avulsion in the Rhine-Meuse

822   delta before historic embankment (The Netherlands). https:// doi.org/10.1130/G45188.1

823   Pierini, J. O., Perillo, G. M. E., Carbone, M. E., & Marini, F. M. (2005). Residual Flow Structure at a Scour-hole in

824   Bahia Blanca Estuary, Argentina. Journal of Coastal Research, 21(4 (214)), 784–796.

825   https://doi.org/10.2112/010-NIS.1

826   Pons, L. J. (1957). De geologie, bodemvorming en de waterstaatkundige ontwikkeling van het Land van Maas en

827   Waal en een gedeelte van het Rijk van Nijmegen. Wageningen University, Wageningen.

828   Rijkswaterstaat. (2005). Stroomwijzer Rijn-Maasmonding. Netherlands: Rijkswaterstaat.

829   Sloff, C. J., van der Ham, G. A., Stouthamer, E., & van Zetten, J. W. (2011). Beheer bodemligging in Spui, Oude

830   Maas en Noord (No. 1203316–000). Deltares.

831   Sloff, C. J., van Spijk, A., Stouthamer, E., & Sieben, A. S. (2013). Understanding and managing the morphology of

832   branches incising into sand-clay deposits in the Dutch Rhine Delta. Intern. J. of Sed. Res., 28, 127–138.

833   Stefani, M., & Vincenzi, S. (2005). The interplay of eustasy, climate and human activity in the late Quaternary

834   depositional evolution and sedimentary architecture of the Po Delta system. Mediterranean Prodelta

835   Systems, 222–223, 19–48. https://doi.org/10.1016/j.margeo.2005.06.029

836   Stouthamer, E., Cohen, K. M., & Gouw, M. J. P. (2011). Avulsion and its implications for fluvial-deltaic

837   architecture: Insights from the Holocene Rhine-Meuse delta. SEPM Special Publication, 97, 215–232.

838   Stouthamer, E., & De Haas, T. (2011). Erodibiliteit en risico op zettingsvloeiing als maat voor stabiliteit van oevers,

839   onderwatertaluds en rivierbodems van de Oude Maas, de Noord en het Spui. Utrecht: Dept. Fysische

840   Geografie / Universiteit Utrecht.

841   Stouthamer, E., Pierik, H. J., & Cohen, K. M. (2011a). Erodibiliteit en kans op het ontstaan van zettingsvloeiing als

842   maat voor stabiliteit van oevers, onderwatertaluds en rivierbodem van de Lek. Universiteit Utrecht &

843   Deltares.

844   Stouthamer, E., Pierik, H. J., & Cohen, K. M. (2011b). Lithologische opbouw van de ondergrond rondom de rivier

845   de Lek. Universiteit Utrecht, Faculty of Geosciences.

846   Stouthamer, Esther, & Berendsen, H. J. A. (2000). Factors Controlling the Holocene Avulsion History of the Rhine-

847   Meuse Delta (The Netherlands). Journal of Sedimentary Research, 70(5), 1051–1064.

848   https://doi.org/10.1306/033000701051

849   TNO. (2010). DINOloket [Internet Portal for Geo-Information]. Retrieved from DINOloket website:

850   www.dinoloket.nl

851   TNO. (2014). DINOloket [Internet Portal for Geo-Information]. Retrieved from DINOloket website:

852   www.dinoloket.nl

853   Törnqvist, T. E., Weerts, H. J. T., & Berendsen, H. J. A. (1994). Definition of two new members in the upper

854   Kreftenheye and Twente Formations (Quaternary, the Netherlands): A final solution to persistent

855   confusion? Geologie En Mijnbouw, 72, 251–264.

856   van der Wegen, M., & Roelvink, J. A. (2012). Reproduction of estuarine bathymetry by means of a process-based

857   model: Western Scheldt case study, the Netherlands. Geomorphology, 179, 152–167.

858   https://doi.org/10.1016/j.geomorph.2012.08.007

859   Vellinga, N. E., Hoitink, A. J. F., van der Vegt, M., Zhang, W., & Hoekstra, P. (2014). Human impacts on tides

860   overwhelm the effect of sea level rise on extreme water levels in the Rhine–Meuse delta. Coastal

861   Engineering, 90, 40–50. https://doi.org/10.1016/j.coastaleng.2014.04.005

862   Vermeulen, B., Hoitink, A. J. F., & Labeur, R. J. (2015). Flow structure caused by a local cross-sectional area

863   increase and curvature in a sharp river bend. Journal of Geophysical Research: Earth Surface, 120(9),

864   1771–1783. https://doi.org/10.1002/2014JF003334

865   Vos, P. C., & Cohen, K. M. (2014). Landschapsgenese en paleogeografie. In BOORrapporten. Twintig meter diep!

866   Mesolithicum in de Yangtzehaven-Maasvlakte te Rotterdam. (pp. 61–146). Moree, J.M., and Sier, M.M.

867   (eds) BOOR Gemeente Rotterdam, Bureau Oudheidkundig Onderzoek Rotterdam, Gemeente Rotterdam.

868   Wang, B., & Xu, Y. J. (2018). Decadal-Scale Riverbed Deformation and Sand Budget of the Last 500 km of the

869   Mississippi River: Insights Into Natural and River Engineering Effects on a Large Alluvial River. Journal

870   of Geophysical Research: Earth Surface, 123(5), 874–890. https://doi.org/10.1029/2017JF004542

871   Wang, C., Yu, X., & Liang, F. (2017). A review of bridge scour: Mechanism, estimation, monitoring and

872   countermeasures. Natural Hazards, 87(3), 1881–1906. https://doi.org/10.1007/s11069-017-2842-2

873   Weerts, H. J. T., & Busschers, F. S. (2003). Beschrijving lithostratigrafische eenheid. Nederlands Instituut voor

874   Toegepaste Geowetenschappen TNO. Utrecht. Retrieved from https://www.dinoloket.nl/stratigrafische-

875   nomenclator/formatie-van-echteld

876   Wiersma, A. P. (2015). De ondergrond van de Boven Merwede, Dordtsche Kil, Nieuwe Maas en Nieuwe Waterweg

877   (No. 1208925-000-ZWS-0024). Deltares.

878   Zimmermann, C., & Kennedy, J. F. (1978). Transverse bed slopes in curved alluvial streams. J. Hydraul. Div.: Proc.

879   ASCE, 104, 33–48.

880